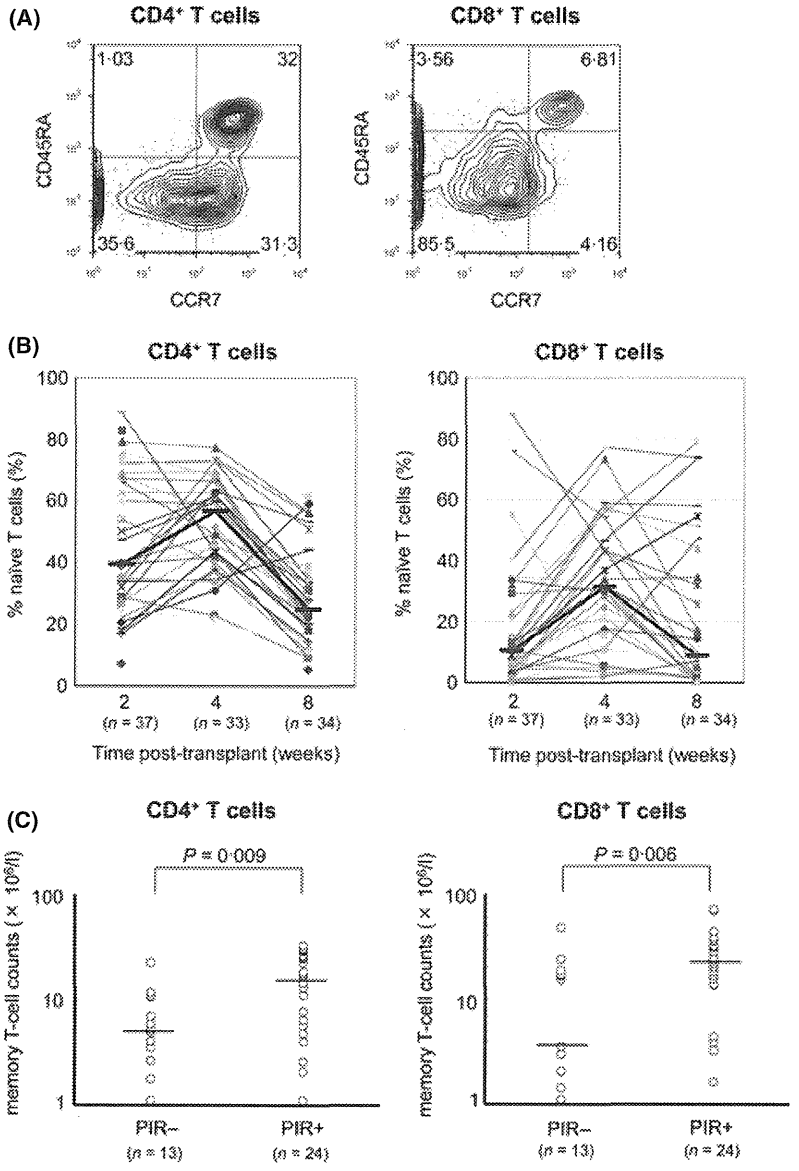

Fig 2. Conversion from naïve to memory T-cell phenotype. (A) A rapid conversion from naïve phenotype ($CD45RA^+CCR7^+$) to memory phenotype ($CD45RA^-CCR7^{+/-}$) in a representative sample at 2 weeks after cord blood transplant (CBT) (Case 5). (B) Relative proportion of naïve $CD4^+$ and $CD8^+$ T cells at 2, 4, and 8 weeks after CBT. Bold horizontal lines denote median values. (C) Memory T-cell counts at 2 weeks after CBT in patients with or without pre-engraftment immune reaction (PIR).

short course of steroid treatment, and none experienced graft failure due to HPS. This observation could be attributed to more intensive immunosuppression from adding mycophenolate mofetil to tacrolimus in the majority of patients (Uchida *et al*, 2011). Although neither the T-cell chimerism nor the memory T-cell counts affected the incidence of acute GVHD, steroid treatment for PIR could suppress the onset of acute GVHD. In conclusion, rapid T-cell chimerism switch and donor-derived memory T-cell expansion were associated with PIR, supporting a significant role of donor-derived T cells in the pathogenesis of the early immune reaction after CBT.

Acknowledgements

The authors thank Madoka Narita for data collection and her skilful secretarial assistance; Eri Watanabe, Mari Muto, and Stephanie Napier for their technical expertise. We also thank all physicians (Shigeyoshi Makino and Hideki Araoka), nurses, pharmacists (Yumiko Uchida and Tadaaki Ito), data managers (Naomi Yamada, Kaori Kobayashi and Rumiko Tsuchihashi), and support personnel for their care of patients involved in this study. This work was supported in part by a Grant-in-Aid from the Japanese Ministry of Health, Labour, and Welfare (H21-Clinical Research-Ippan-020).

Author contributions

NM, HY, NW, HN, and ST designed the study; NM, HY, and NW performed the research; NM and HY analysed data; HY, NU, HO, AN, TI, K Ishiwata, NN, MT, Y A-M, K Izutsu, KM, AW, and ST performed transplantation; AY reviewed histopathological findings; and NM, HY, NW, NU, HN, and ST contributed to writing the paper.

Competing interests

The authors have no competing interests.

Naofumi Matsuno[1,2]*
Hisashi Yamamoto[2]*
Nobukazu Watanabe[1]
Naoyuki Uchida[2]
Hikari Ota[2]
Aya Nishida[2]
Taichi Ikebe[2]
Kazuya Ishiwata[2]
Nobuaki Nakano[2]
Masanori Tsuji[2]
Yuki Asano-Mori[2]
Koji Izutsu[2]
Kazuhiro Masuoka[2]
Atsushi Wake[2]
Akiko Yoneyama[3]
Hiromitsu Nakauchi[4]
Shuichi Taniguchi[2,5]

[1]*Laboratory of Diagnostic Medicine, Division of Stem Cell Therapy, Centre for Stem Cell Biology and Regenerative Medicine, the Institute of Medical Science, the University of Tokyo, Tokyo, Japan,* [2]*Department of Haematology, Toranomon Hospital, Tokyo, Japan,* [3]*Department of Infectious Diseases, Toranomon Hospital, Tokyo, Japan,* [4]*Division of Stem Cell Therapy, Centre for Stem Cell Biology and Regenerative Medicine, the Institute of Medical Science, the University of Tokyo, Tokyo, Japan and* [5]*Okinaka Memorial Institute for Medical Research, Tokyo, Japan*
E-mail: nwatanab@ims.u-tokyo.ac.jp

*The first two authors contributed equally to this work.

Keywords: cord blood transplantation, chimerism, human leucocyte antigen-Flow method, naïve and memory T-cell, pre-engraftment immune reaction.

First published online 1 November 2012
doi: 10.1111/bjh.12097

Supporting Information

Additional Supporting Information may be found in the online version of this article:

Table SI. Patient and cord blood characteristics.

Please note: Wiley-Blackwell are not responsible for the content or functionality of any supporting materials supplied by the authors. Any queries (other than missing material) should be directed to the corresponding author for the article.

References

Frangoul, H., Wang, L., Harrell, F.E., Jr, Ho, R. & Domm, J. (2009) Preengraftment syndrome after unrelated cord blood transplant is a strong predictor of acute and chronic graft-*versus*-host disease. *Biology of Blood and Marrow Transplantation*, **15**, 1485–1488.

Grindebacke, H., Stenstad, H., Quiding-Jarbrink, M., Waldenstrom, J., Adlerberth, I., Wold, A.E. & Rudin, A. (2009) Dynamic development of homing receptor expression and memory cell differentiation of infant CD4+CD25high regulatory T cells. *Journal of Immunology*, **183**, 4360–4370.

Gutman, J.A., Turtle, C.J., Manley, T.J., Heimfeld, S., Bernstein, I.D., Riddell, S.R. & Delaney, C. (2010) Single-unit dominance after double-unit umbilical cord blood transplantation coincides with a specific CD8+ T-cell response against the nonengrafted unit. *Blood*, **115**, 757–765.

Kishi, Y., Kami, M., Miyakoshi, S., Kanda, Y., Murashige, N., Teshima, T., Kusumi, E., Hara, S., Matsumura, T., Yuji, K., Masuoka, K., Wake, A., Morinaga, S., Kanemaru, M., Hayashi, T., Tanaka, Y. & Taniguchi, S. (2005) Early immune reaction after reduced-intensity cord-blood transplantation for adult patients. *Transplantation*, **80**, 34–40.

Matsuno, N., Wake, A., Uchida, N., Ishiwata, K., Araoka, H., Takagi, S., Tsuji, M., Yamamoto, H., Kato, D., Matsuhashi, Y., Seo, S., Masuoka, K., Miyakoshi, S., Makino, S., Yoneyama, A., Kanda, Y. & Taniguchi, S. (2009) Impact of HLA disparity in the graft-*versus*-host direction on engraftment in adult patients receiving reduced-intensity cord blood transplantation. *Blood*, **114**, 1689–1695.

Narimatsu, H., Terakura, S., Matsuo, K., Oba, T., Uchida, T., Iida, H., Hamaguchi, M., Watanabe, M., Kohno, A., Murata, M., Sawa, M., Miyamura, K. & Morishita, Y. (2007) Short-term methotrexate could reduce early immune reactions and improve outcomes in umbilical cord blood transplantation for adults. *Bone Marrow Transplantation*, **39**, 31–39.

Patel, K.J., Rice, R.D., Hawke, R., Abboud, M., Heller, G., Scaradavou, A., Young, J.W. & Barker, J.N. (2010) Pre-engraftment syndrome after double-unit cord blood transplantation: a distinct syndrome not associated with acute graft-*versus*-host disease. *Biology of Blood and Marrow Transplantation*, **16**, 435–440.

Takagi, S., Masuoka, K., Uchida, N., Ishiwata, K., Araoka, H., Tsuji, M., Yamamoto, H., Kato, D., Matsuhashi, Y., Kusumi, E., Ota, Y., Seo, S., Matsumura, T., Matsuno, N., Wake, A., Miyakoshi, S., Makino, S., Ohashi, K., Yoneyama, A. & Taniguchi, S. (2009) High incidence of haemophagocytic syndrome following umbilical cord blood transplantation for adults. *British Journal of Haematology*, **147**, 543–553.

Uchida, N., Wake, A., Nakano, N., Ishiwata, K., Takagi, S., Tsuji, M., Yamamoto, H., Kato, D., Matsuno, N., Masuoka, K., Araoka, H., Asano-Mori, Y., Izutsu, K., Makino, S., Yoneyama, A. & Taniguchi, S. (2011) Mycophenolate and tacrolimus for graft-*versus*-host disease prophylaxis for elderly after cord blood transplantation: a matched pair comparison with tacrolimus alone. *Transplantation*, **92**, 366–371.

Watanabe, N., Takahashi, S., Ishige, M., Ishii, Y., Ooi, J., Tomonari, A., Tsukada, N., Konuma, T., Kato, S., Sato, A., Tojo, A. & Nakauchi, H. (2008) Recipient-derived cells after cord blood transplantation: dynamics elucidated by multicolour FACS, reflecting graft failure and relapse. *Biology of Blood and Marrow Transplantation*, **14**, 693–701.

Membrane-bound human SCF/KL promotes in vivo human hematopoietic engraftment and myeloid differentiation

Shinsuke Takagi,[1-3] Yoriko Saito,[1] Atsushi Hijikata,[4] Satoshi Tanaka,[1,5,6] Takashi Watanabe,[4] Takanori Hasegawa,[7] Shinobu Mochizuki,[7] Jun Kunisawa,[5] Hiroshi Kiyono,[5] Haruhiko Koseki,[7] Osamu Ohara,[4,8] Takashi Saito,[3,9] Shuichi Taniguchi,[2] Leonard D. Shultz,[10] and Fumihiko Ishikawa[1]

[1]Research Unit for Human Disease Models, RIKEN Research Center for Allergy and Immunology, Yokohama, Japan; [2]Department of Hematology, Toranomon Hospital, Tokyo, Japan; [3]Department of Immune Regulation Research, Chiba University of Medical and Pharmaceutical Sciences, Chiba, Japan; [4]Laboratory for Immunogenomics, RIKEN Research Center for Allergy and Immunology, Yokohama, Japan; [5]Division of Mucosal Immunology, Institute of Medical Science, University of Tokyo, Tokyo, Japan; [6]Nippon Becton Dickinson Company, Tokyo, Japan; [7]Laboratory for Developmental Genetics, RIKEN Research Center for Allergy and Immunology, Yokohama, Japan; [8]Department of Human Gene Research, Kazusa DNA Research Institute, Kisarazu, Japan; [9]Laboratory for Cell Signaling, RIKEN Research Center for Allergy and Immunology, Yokohama, Japan; and [10]The Jackson Laboratory, Bar Harbor, ME

In recent years, advances in the humanized mouse system have led to significantly increased levels of human hematopoietic stem cell (HSC) engraftment. The remaining limitations in human HSC engraftment and function include lymphoid-skewed differentiation and inefficient myeloid development in the recipients. Limited human HSC function may partially be attributed to the inability of the host mouse microenvironment to provide sufficient support to human hematopoiesis. To address this problem, we created membrane-bound human stem cell factor (SCF)/KIT ligand (KL)–expressing NOD/SCID/IL2rgKO (hSCF Tg NSG) mice. hSCF Tg NSG recipients of human HSCs showed higher levels of both human CD45$^+$ cell engraftment and human CD45$^+$CD33$^+$ myeloid development compared with NSG recipients. Expression of hSCF/hKL accelerated the differentiation of the human granulocyte lineage cells in the recipient bone marrow. Human mast cells were identified in bone marrow, spleen, and gastrointestinal tissues of the hSCF Tg NSG recipients. This novel in vivo humanized mouse model demonstrates the essential role of membrane-bound hSCF in human myeloid development. Moreover, the hSCF Tg NSG humanized recipients may facilitate investigation of in vivo differentiation, migration, function, and pathology of human mast cells. (*Blood*. 2012;119(12): 2768-2777)

Introduction

The humanized mouse system, a xenogeneic transplantation and engraftment model for human hematopoietic stem cells (HSCs) and peripheral blood (PB) mononuclear cells (MNCs), facilitates the investigation of human hematopoietic and immune systems in vivo.[1,2] Since the pioneering work using SCID-hu[3] and Hu-PBL-SCID models,[4] investigators have attempted to better recapitulate human biology in mice across xenogeneic immunologic barriers. Recently, the introduction of targeted null mutations of immune-related genes, such as *Rag1, Rag2, Il2rg*, or *Prf1* in recipient mice, has improved engraftment levels of human CD45$^+$ leukocytes.[2,5-9] However, limitations remain in the ability of the host mouse hematopoietic microenvironment to support human hematopoiesis. The impaired development of human T-lymphoid and myeloid lineage cells compared with human B-lymphoid lineage cells in NOD/SCID and other immune-compromised mice may be the result of the lack of appropriate microenvironmental support. The recently created human leukocyte antigen (HLA) class I expressing immune-compromised NOD/SCID/IL2r γ null (NSG) mice partially addresses this issue for human T-cell development. Human CD8$^+$ T cells developing within these recipients of transplanted human HSCs exhibited cytokine production and cytotoxicity in an HLA-restricted manner.[10-12]

To create a hematopoietic microenvironment more suitable for human myeloid development, we developed a new immune-compromised mouse strain that expresses human membrane bound stem cell factor (SCF) under the control of the phosphoglycerate kinase (PGK) promoter (hSCF Tg NSG). Using hSCF Tg NSG mice as recipients of human HSCs, we aimed to clarify the role of membrane-bound form of SCF in supporting the engraftment of human hematopoietic cells and influencing the differentiation of the human myeloid lineage in the recipient mouse BM, spleen, and other organs. Here we show nearly complete human hematopoietic chimerism in the BM of hSCF Tg NSG recipients. In the BM of these recipients, human granulocytes accounted for the majority of engrafted human cells reflecting the physiologic human BM status. In addition to the development of immature and mature granulocytes, c-Kit$^+$ human mast cells differentiated efficiently in BM, spleen, and mucosal tissues. The hSCF Tg NSG mice, by supporting efficient human myeloid development including mast cells, may serve as a novel platform for in vivo investigation of human mast cell development and allergic responses.

Methods

Mice

NOD.Cg-*Prkdc*^{scid} *IL2rg*^{tm1Wjl} (NSG) mice and NOD.Cg-*Prkdc*^{scid} *IL2rg*^{tm1Wjl} Tg(PGK1-KITLG*220)441Daw/J, abbreviated as hSCF Tg NSG mice,

Submitted May 6, 2011; accepted October 2, 2011. Prepublished online as *Blood* First Edition paper, January 25, 2012; DOI 10.1182/blood-2011-05-353201.

The online version of this article contains a data supplement.

The publication costs of this article were defrayed in part by page charge payment. Therefore, and solely to indicate this fact, this article is hereby marked "advertisement" in accordance with 18 USC section 1734.

were generated at The Jackson Laboratory. The human membrane-bound SCF transgene driven by the human PGK promoter was backcrossed more than 10 generations from the original C3H/HeJ strain background[13] onto the NSG strain. All the mice were bred and maintained at The Jackson Laboratory and animal facility at RIKEN RCAI under defined flora according to guidelines established and approved by the Institutional Animal Committees at each respective institution.

Purification and transplantation of human HSCs

All experiments were performed with authorization from the Institutional Review Board for Human Research at RIKEN RCAI. Cord blood (CB) samples were first processed for isolation of MNCs using LSM lymphocyte separation medium (MP Biomedicals). CB MNCs were then enriched for human $CD34^+$ cells using anti–human CD34 microbeads (Miltenyi Biotec) and sorted for 7-AAD^- lineage (hCD3/hCD4/hCD8/hCD19/hCD56)$^-CD34^+CD38^-$ HSCs using FACSAria (BD Biosciences). To achieve high purity of donor HSCs, doublets were excluded by analysis of forward scatter (FSC)–height/FSC-width and side scatter (SSC)-height/SSC-width. Purity of each sorted sample was higher than 95%. Newborn (within 2 days of birth) hSCF Tg and non-Tg NSG recipients received 150 cGy total body irradiation using a ^{137}Cs-source irradiator, followed by intravenous injection of 5×10^2 to 5.3×10^4 sorted HSCs via the facial vein.

Analysis of human cell engraftment by flow cytometry

The recipient PB harvested from the retro-orbital plexus was evaluated for human hematopoietic engraftment every 3 to 4 weeks starting at 4 to 6 weeks after transplantation. After lysis of erythrocytes, cells were stained with anti-hCD45, anti-msCD45, anti-hCD3, anti-hCD19, anti-hCD33, and anti-hCD56 to determine human hematopoietic chimerism and to analyze cell lineages engrafted in the recipients. At 8 to 35 weeks after transplantation, the recipients were killed and single-cell suspensions of BM and spleen were analyzed using flow cytometry. Antibodies used for flow cytometry are specified in supplemental Methods (available on the *Blood* Web site; see the Supplemental Materials link at the top of the online article). The labeled cells were analyzed using FACSCantoII or FACSAria (BD Biosciences).

Morphologic analysis of cytospin specimens

Cytospin specimens of FACS-purified human myeloid cells were prepared with a Shandon Cytospin 4 cytocentrifuge (Thermo Electric) using standard procedures. To identify nuclear and cytoplasmic characteristics of each myeloid cell, cytospin specimens were stained with 100% May-Grünwald solution (Merck) for 3 minutes, followed by 50% May-Grünwald solution in phosphate buffer (Merck) for additional 5 minutes, and then with 5% Giemsa solution (Merck) in phosphate buffer for 15 minutes. All staining procedures were performed at room temperature. Light microscopy was performed with Zeiss Axiovert 200 (Carl Zeiss).

Microarray analysis

Purified $hCD45^+CD33^+$c-$Kit^-CD203c^-$HLA-DR^- granulocytes and $hCD45^+CD33^+$ c-$Kit^-CD203c^-$HLA-DR^+CD14^+ monocytes from BM of 4 hSCF Tg NSG recipients and 3 non-Tg NSG recipients as well as neutrophils and monocytes from 2 healthy persons were evaluated using Human Genome U133 plus Version 2.0 GeneChips (Affymetrix). Total RNA was extracted with TRIzol (Invitrogen) from more than 10^4 sorted cells and amplified to cDNA using the Ovation Pico WTA System (Nugen). Biotinylated cDNA was synthesized with Two-Cycle Target Labeling Kit (Affymetrix). Microarray data were analyzed using the Bioconductor package (Bioconductor; http://www.bioconductor.org). The signal intensities of the probe sets were normalized using the GC-RMA program (Bioconductor). The RankProd program was used to select differentially expressed genes with a cutoff P value of less than .01 and an estimated false-positive rate of less than 0.05.[14] Gene annotation was obtained from Ingenuity Pathway Analysis and Gene Ontology Annotation databases (Ingenuity systems, http://www.ingenuity.com; Gene Ontology Annotation, http://www.ebi.ac.up/GOA). For differentially transcribed genes, GO term enrichment analysis was performed according to a method described by Draghici et al[15] with a correction of multiple testing using false discovery rate.[16] Eventually, GO terms with the false discovery rate-corrected P value $< .05$ were selected as functionally enriched terms. Raw data for microarray data are accessible at the RefDIC database (http://refdic.rcai.riken.jp) under the following accession numbers: RSM06616, RSM06617, RSM06618, RSM06620, RSM06621, RSM06622, RSM06623, RSM06633, RSM06642, RSM06648, RSM06665, RSM06667, RSM06668, RSM06669, RSM06670, RSM08241, and RSM08243. Differences in expression levels were considered significant if P is $< .05$ using Kruskal-Wallis, Wilcoxon-Mann-Whitney, or Student t test in KaleidaGraph (Synergy Software).

IHC and immunofluorescence imaging

Thin (~ 5-μm) sections prepared from paraformaldehyde-fixed paraffin-embedded tissues were stained with H&E using standard procedures. Immunohistochemistry (IHC) and immunofluorescence labeling were performed using standard procedures. Antibodies used for IHC and immunofluorescence labeling were mouse anti–human mast cell tryptase monoclonal antibody (Dako North America, clone AA1), mouse anti–human CD45 monoclonal antibody (Dako North America, clone $2B11^+PD7/26$), rabbit anti–human CD117 monoclonal antibody (Epitomics, clone YR145), and rabbit anti–human CD14 polyclonal antibody (Atlas Antibodies). Light microscopy was performed using an Axiovert 200 (Carl Zeiss). For quantification of $tryptase^+$ cell frequency, 3 high-power fields from 3 different recipients were examined using AutoMeasure module of AxioVision software (Release 4, Carl Zeiss). Confocal microscopy was performed using a LSM710 equipped with C-APOCHROMAT 40×/1.2 (Carl Zeiss).

Results

Human hematopoietic repopulation is enhanced in hSCF Tg NSG recipients

The humanized mouse model system has served as a tool to investigate human hematopoiesis, immunity, and diseases in vivo. However, one of the major limitations in the system is that the microenvironment supporting human hematopoiesis and immunity is primarily of mouse origin. In the present study, we created a strain of NSG mice expressing membrane-bound human SCF to analyze the role of the BM microenvironment in human hematopoietic lineage determination and development.

c-Kit, the receptor for SCF, is expressed at lower levels in human CB $Lin^-CD34^+CD38^-$ early HSCs and at high levels in mast cells.[17-19] For reconstitution of human myeloid and lymphoid cells, 5×10^2 to 5.3×10^4 FACS-purified CB $Lin^-CD34^+CD38^-$ HSCs were transplanted into newborn sublethally irradiated (1.5 Gy) hSCF Tg NSG mice and into non-Tg NSG controls (Table 1). To determine the kinetics of human hematopoietic chimerism in the recipient circulation, we performed flow cytometric analysis of PB every 3 to 4 weeks starting at 4 to 6 weeks after transplantation. During long-term observation, all the 21 hSCF Tg NSG recipient mice became moribund at 8 to 35 weeks after transplantation. Complete blood count analysis demonstrated reduced erythrocyte hemoglobin concentration in the PB of hSCF Tg NSG recipients compared with non-Tg NSG recipients (Figure 1A). Anemia in hSCF Tg NSG recipients was not associated with abnormalities in mean corpuscular volume, mean corpuscular hemoglobin, or mean corpuscular hemoglobin concentration (supplemental Figure 1). The suppression of host erythropoiesis in the hSCF Tg NSG recipients was related to the irradiation and engraftment of the human HSCs because unmanipulated nontransplanted hSCF Tg NSG mice did not develop anemia (supplemental Figure 1).

Table 1. Summary of hSCF Tg NSG and non-Tg NSG recipients analyzed

Recipient ID	CB ID	Graft dose	Survival, wks	CBC at time of death					% chimerism at time of death			% of CD45+ in BM				% of CD33+ in BM			% of CD45+ in BM			% chimerism of erythroid cells in BM
				WBC, $\times 10^3$/L	RBC, $\times 10^4/\mu$L	Hemoglobin, g/dL	Hematocrit, %	Platelets, $\times 10^3/\mu$L	PB	BM	Spleen	CD33+	CD3+	CD19+	CD3−CD56+	CD117+CD203c+	HLA DR−	HLA DR+	CD117+CD203c+	HLA DR−	HLA DR+	
N1-1	1	5000	21	1.1	500	10.0	35.0	550	75.5	93.3	95.3	31.1	1.2	50.2	0.3	0.9	51.5	47.6	0.3	16.0	14.8	NA
N1-2	1	5000	16	1.4	730	13.0	44.0	1100	42.6	76.1	72.9	35.2	0.1	54.8	0.4	0.7	39.6	59.7	0.2	13.9	21.0	NA
N1-3	1	5000	24	NA	NA	NA	NA	NA	20.7	12.6	4.4	32.9	3.8	60.7	0.0	4.4	37.9	57.7	1.0	12.5	19.0	3.1
S1-1	1	5000	23	4.1	220	6.7	15.6	150	99.1	99.7	94.4	77.2	24.5	19.2	0.5	3.9	80.6	15.5	3.0	62.2	11.9	NA
S1-2	1	5000	20	6.8	220	5.0	18.0	30	83.2	99.4	97.7	75.5	2.6	28.4	0.3	6.7	68.7	24.6	5.1	51.8	18.6	36.3
S1-3	1	5000	21	0.7	320	7.0	25.0	330	76.9	99.7	95.8	70.9	1.5	16.6	0.2	14.6	50.0	35.4	10.4	35.5	25.1	0.0
S1-4	1	500	26	0.5	150	3.0	11.0	250	30.7	97.0	86.3	69.0	2.0	47.5	0.1	6.9	68.6	24.5	4.8	47.3	16.9	NA
N2-1	2	10 000	35	0.8	390	8.0	30.0	110	31.7	54.9	87.1	50.3	21.8	25.8	2.4	19.1	7.4	73.5	9.6	3.7	37.0	11.5
S2-1	2	10 000	16	1.3	186	4.1	13.2	583	90.7	96.6	99.3	18.7	3.2	40.6	1.2	34.4	18.0	47.6	6.4	3.4	8.9	NA
S3-1	3	10 000	13	0.2	215	3.9	12.6	793	52.0	97.8	90.9	54.2	0.0	42.8	0.7	19.0	44.6	36.4	10.3	24.2	19.7	NA
S3-2	3	10 000	15	2.2	161	3.1	9.8	458	93.6	99.6	98.2	61.5	4.4	20.4	1.4	7.3	60.5	32.2	4.5	37.2	19.8	NA
S4-1	4	10 000	13	0.5	97	1.9	5.1	6	98.6	100.0	98.2	52.0	1.2	39.8	0.3	2.7	81.9	15.4	1.4	42.6	8.0	27.2
N5-1	5	12 000	35	3.1	310	7.0	25.0	550	6.8	36.8	48.9	29.9	17.5	41.9	NA	22.6	7.0	70.4	6.8	2.1	21.1	5.8
N6-1	6	14 000	23	2.1	520	10.0	34.0	620	57.6	65.0	83.6	29.3	17.6	43.1	1.6	3.3	45.1	51.6	1.0	13.2	15.1	7.4
N6-2	6	14 000	21	1.6	680	12.0	40.0	660	64.6	25.3	81.5	10.4	17.2	64.4	0.5	33.9	17.5	48.6	3.5	1.8	5.1	1.4
N6-3	6	14 000	24	2.3	490	10.0	33.0	80	73.8	71.8	92.8	18.5	13.9	51.1	0.8	10.6	8.5	81.4	2.0	1.6	15.1	12.8
S6-1	6	14 000	16	2.2	236	4.5	15.5	33	70.0	88.5	94.7	39.4	5.8	43.6	0.7	68.9	8.1	23.0	27.1	3.2	9.1	33.1
S6-2	6	14 000	14	4.6	270	6.0	21.0	108	85.4	90.0	95.2	33.3	11.6	46.8	0.9	36.5	16.0	47.5	12.2	5.3	15.8	5.8
S7-1	7	15 000	16	4.9	293	6.1	19.4	132	93.6	99.7	98.8	76.5	1.4	42.3	0.6	1.6	80.1	18.3	1.2	61.3	14.0	NA
S8-1	8	16 000	13	1.0	183	3.3	9.4	78	98.6	100.0	99.7	16.2	19.9	52.1	0.9	25.1	1.0	73.9	4.1	0.2	12.0	NA
S8-2	8	16 000	11	1.0	376	5.6	18.4	568	89.5	99.6	98.5	48.6	0.2	54.5	0.6	4.9	42.0	53.1	2.4	20.4	25.8	NA
N9-1	9	18 000	20	2.7	650	13.0	42.0	130	71.6	87.2	92.0	15.0	1.7	72.4	0.4	1.4	24.7	74.0	0.2	3.7	11.1	9.8
S9-1	9	18 000	16	1.4	164	3.4	10.6	80	90.4	99.9	97.0	51.4	0.2	35.1	0.2	2.4	54.9	42.7	1.2	28.2	21.9	25.5
N10-1	10	20 000	19	1.0	660	12.0	42.0	77	38.4	46.5	87.1	25.9	44.4	24.1	0.8	3.9	6.2	89.9	1.0	1.6	23.3	12.0
N10-2	10	20 000	14	NA	NA	NA	NA	NA	NA	NA	NA	NA	NA	NA	NA	NA	NA	NA	NA	NA	NA	NA
N10-3	10	20 000	12	NA	NA	NA	NA	NA	NA	NA	NA	NA	NA	NA	NA	NA	NA	NA	NA	NA	NA	NA
S10-1	10	20 000	19	2.5	292	6.1	20.9	6	95.5	99.7	97.3	42.3	14.4	35.5	0.9	5.7	28.8	65.5	2.4	12.2	27.7	4.3
S10-2	10	20 000	14	1.5	170	3.0	11.0	30	95.8	99.7	89.3	27.3	28.4	28.0	5.4	18.6	19.8	61.6	5.1	5.4	16.8	17.1
N11-1	11	36 000	20	25.1	470	9.0	31.0	240	84.1	70.7	94.0	19.5	5.9	63.6	0.7	3.8	17.8	78.4	0.7	3.5	15.3	42.3
S11-1	11	36 000	10	19.2	420	8.0	27.0	410	77.5	98.0	95.3	34.0	0.2	43.5	0.5	4.5	34.6	60.9	1.5	11.8	20.7	58.5
N12-1	12	53 000	8	NA	NA	NA	NA	NA	36.9	95.6	83.3	20.3	0.0	72.2	0.2	NA	NA	NA	NA	NA	NA	NA
S12-1	12	53 000	11	NA	NA	NA	NA	NA	100.0	100.0	99.9	43.5	6.5	39.1	1.5	NA	NA	NA	NA	NA	NA	NA
S12-2	12	53 000	8	NA	NA	NA	NA	NA	93.1	100.0	NA	65.6	0.2	13.2	NA	1.6	83.7	14.7	1.0	54.9	9.6	NA
S12-3	12	53 000	13	13.6	211	3.9	10.9	165	57.0	79.5	68.3	47.5	12.5	35.7	2.2	8.8	59.9	31.3	4.2	28.5	14.9	NA
N13-1	13	17 000	20	6.4	720	13.0	45.0	470	39.2	85.0	81.8	21.8	0.0	69.0	0.2	0.4	46.1	53.5	0.1	10.0	11.7	7.6
S13-1	13	17 000	20	2.8	290	7.0	27.0	510	74.9	93.7	94.5	38.1	6.0	47.8	0.4	26.6	31.3	42.1	10.1	11.9	16.0	48.4

A total of 21 human HSC-engrafted hSCFTg NSG (S) recipients and 15 human HSC-engrafted non-Tg NSG (N) recipients were created.
WBC indicates white blood cell count; RBC, red blood cell count; and NA, not applicable.

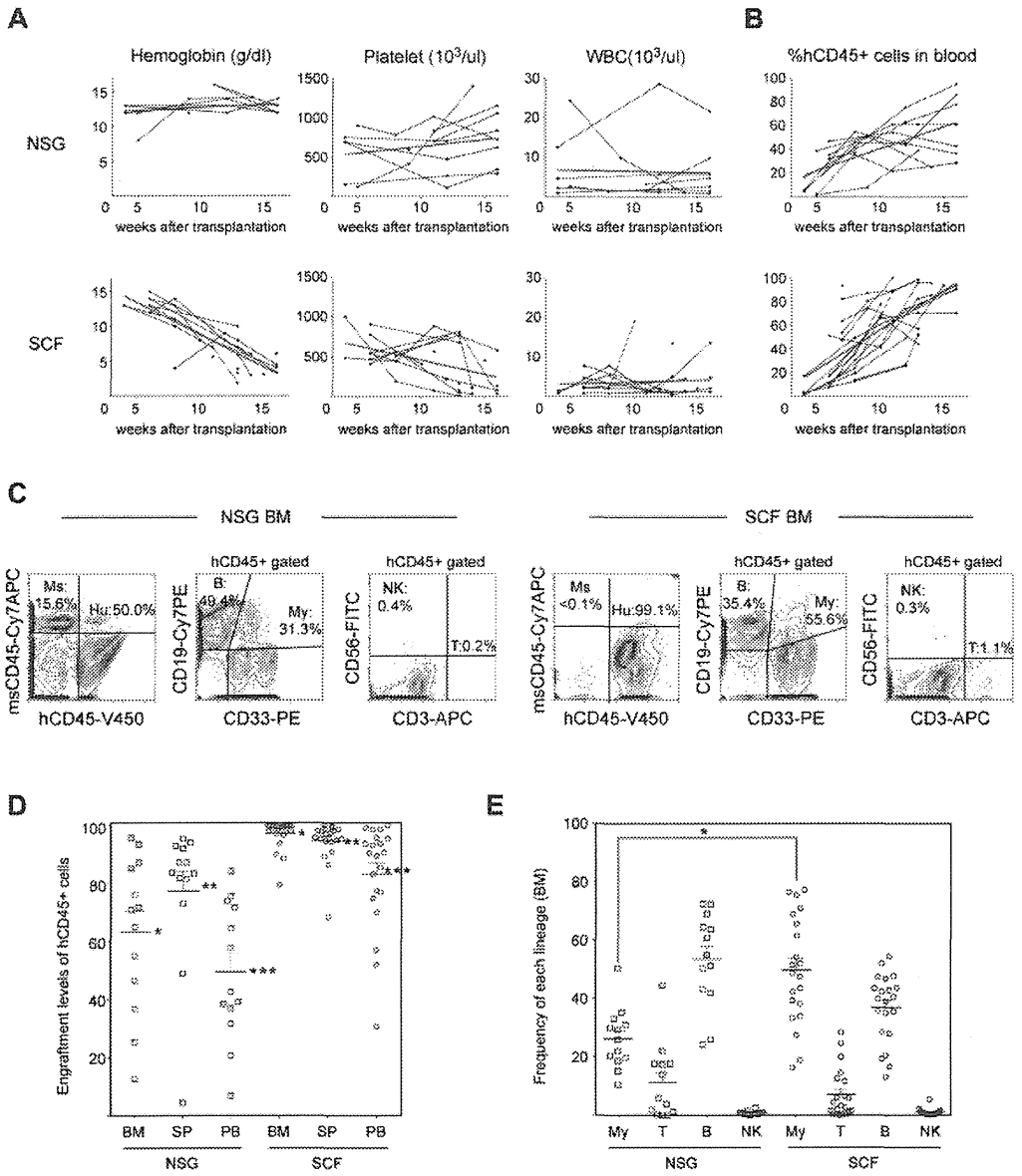

Figure 1. Human hematopoietic engraftment is enhanced in hSCF Tg NSG recipients. (A) hSCF Tg NSG recipients developed progressive anemia as evidenced by reduced hemoglobin concentration compared with non-Tg NSG mice transplanted with human HSCs from the same donor source. (B) Human CD45$^+$ chimerism was analyzed over time in PB of hSCF Tg and non-Tg NSG recipients. (C) Representative flow cytometric contour plots demonstrating the presence of human CD45$^+$ cells, CD19$^+$ B cells, CD33$^+$ myeloid cells, CD3$^+$ T cells, and CD56$^+$CD3$^-$ NK cells in recipient BM. (D) At the time of death, engraftment levels of human CD45$^+$ cells in the BM, spleen, and PB of hSCF Tg NSG recipients were significantly higher compared with non-Tg NSG controls (BM: hSCF Tg n = 21, non-Tg n = 13, $P < .0001$; spleen: hSCF Tg n = 21, non-Tg n = 13, $P = .0065$; PB: hSCF Tg n = 21, non-Tg n = 13, $P < .0001$). (E) In hSCF Tg NSG recipient BM, significantly greater human CD33$^+$ myeloid lineage development was observed (hSCF Tg n = 21, non-Tg n = 13, $P = .0002$).

Impaired mouse erythropoiesis in these engrafted hSCF Tg NSG mice was associated with rapid expansion of hCD45$^+$ hematopoietic cells compared with non-Tg NSG recipients (Figure 1B).

At 8 to 35 weeks after transplantation, individual hSCF Tg NSG recipients were analyzed to determine levels of reconstitution of human hematopoiesis and immunity in the BM, spleen, and PB. At the time of necropsy, we did not observe any gross macroscopic abnormalities in these recipients. We performed flow cytometric analysis to evaluate the engraftment levels of human CD45$^+$ cells (calculated as % hCD45$^+$ cells relative to total numbers of mouse and human CD45$^+$ cells in the nucleated cell gate). Engraftment levels of human CD45$^+$ leukocytes in the BM, spleen, and PB were significantly higher in hSCF Tg NSG recipients (mean ± SEM; 97.1% ± 1.1%, 94.5% ± 1.6%, and 83.1% ± 3.9%, respectively; n = 21) compared with engrafted non-Tg NSG recipients (63.1% ± 7.3%, 77.3% ± 6.9%, and 49.5% ± 6.5%, respectively; n = 13; $P < .0001$, $P = .0065$, and $P < .0001$ by 2-tailed t test, respectively; Figure 1C-D). Compared with enhanced engraftment of human leukocytes in the recipient BM, development of human erythroid precursors was not significantly different in hSCF Tg NSG recipients compared with non-Tg NSG recipients (hSCFTg: 25.6% ± 6.1%; n = 10 and non-Tg NSG controls: 11.4% ± 3.6%; n = 10; $P = .0601$; supplemental Figure 2). We next analyzed the development of human lymphoid and myeloid cells in the engrafted human CD45$^+$ hematopoietic cell populations by flow cytometry using monoclonal antibodies against hCD3, hCD19,

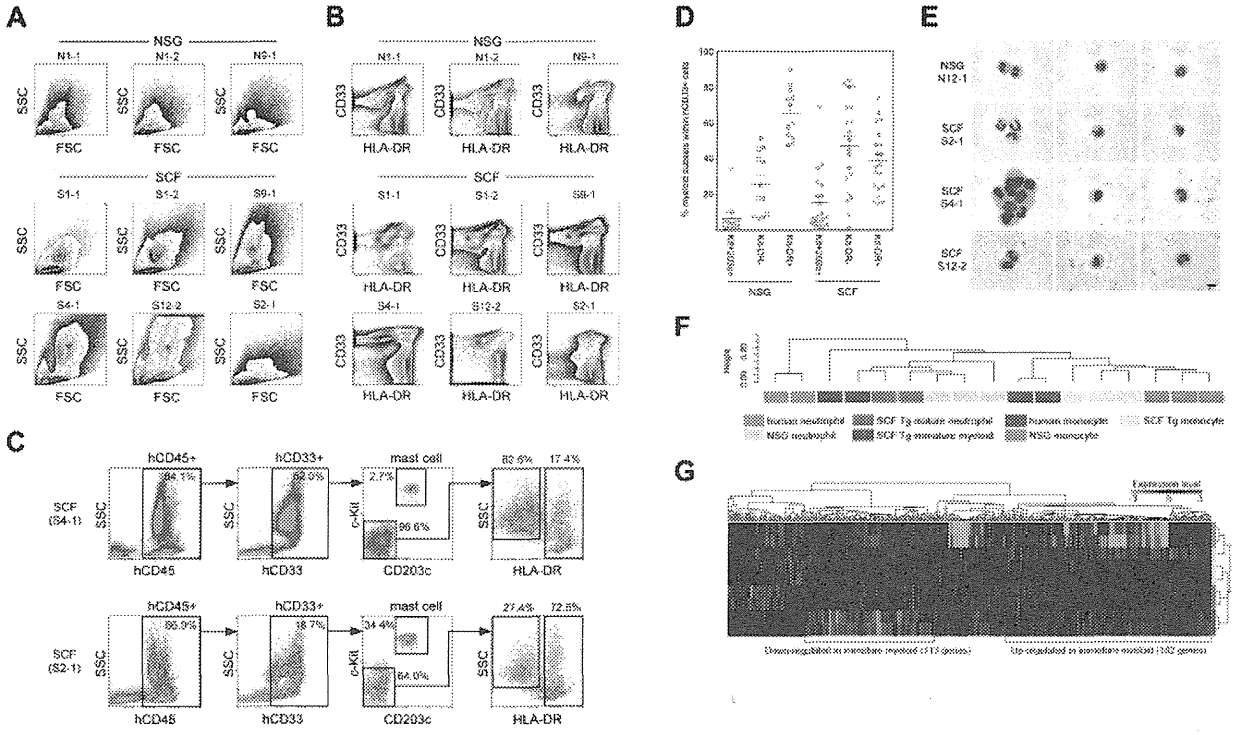

Figure 2. HLA-DR-negative human myeloid cells predominate in hSCF Tg NSG recipient BM. (A) Flow cytometric contour plots demonstrating FSC and SSC characteristics of 6 hSCF Tg NSG recipient BM (S1-1, S1-2, S9-1, S4-1, S12-2, and S2-1) and 3 non-Tg NSG recipient BM (N1-1, N1-2, and N9-1). Polymorphonuclear myeloid cells (red asterisks) are present at high frequencies in hSCF Tg NSG recipient BM. (B) Flow cytometry contour plots demonstrating hCD33 and HLA-DR expression in the same recipients as shown in panel A. Consistent with their FSC and SSC characteristics, hSCF Tg NSG recipient BM contained a prominent $CD33^+HLA\text{-}DR^-$ granulocyte population (red asterisks; N1-1, killed at 21 weeks; N1-2, killed at 16 weeks; N9-1, killed at 20 weeks; S1-1, killed at 23 weeks; S1-2, killed at 20 weeks; S9-1, killed at 16 weeks; S4-1, killed at 13 weeks; S12-2, killed at 8 weeks; and S2-1, killed at 16 weeks). (C) Representative flow cytometric scatter plots of hSCF Tg NSG recipient BM demonstrating the identification of human $c\text{-}Kit^+CD203c^+$ mast cells within the $hCD33^+$ fraction and $HLA\text{-}DR^-SSC^{high}$ granulocytes and $HLA\text{-}DR^+SSC^{low}$ APCs within the $c\text{-}Kit^-CD203c^-$ fraction (S4-1, killed at 13 weeks; and S2-1, killed at 16 weeks). (D) Frequencies of human $c\text{-}Kit^+CD203c^+$ mast cells, $CD33^+HLA\text{-}DR^-$ granulocytes, and $CD33^+HLA\text{-}DR^+$ APCs within the total $hCD45^+hCD33^+$ myeloid cell population in the BM of hSCF Tg and non-Tg NSG recipients. Numbers of cells in the granulocyte/neutrophil fraction were significantly higher in hSCF Tg NSG recipient BM (hSCF Tg n = 20, non-Tg n = 12, $P = .0001$). (E) $CD33^+HLA\text{-}DR^-$ cells from hSCF Tg and non-Tg NSG recipient BM were FACS-purified and examined by MGG staining. In 9 of 13 hSCF Tg recipients (S4-1 and S12-2 shown as representative), immature myeloid cells composed the majority of cells in this fraction. In 4 of 13 hSCF Tg recipients (S2-1 shown as representative) and 4 of 5 non-Tg NSG recipients (N12-1 shown as representative), mature neutrophils (band and segmented forms) were observed (N12-1, killed at 8 weeks; S2-1, killed at 16 weeks; S4-1, killed at 13 weeks; and S12-2, killed at 8 weeks). (F-G) Global transcriptional profiles of FACS-purified $CD33^+cKit^-CD203^-HLA\text{-}DR^-$ granulocytes and $CD33^+c\text{-}Kit^-CD203c^-HLA\text{-}DR^+CD14^+$ monocytes derived from hSCF Tg NSG and non-Tg NSG recipient BM as well as human $CD16^+$ neutrophils and $CD14^+$ monocytes were compared. (F) Unsupervised clustering for each group is shown. (G) The expression heatmap demonstrates genes that are significantly under- and over-represented in each population.

hCD56, and hCD33 along with anti–human and anti–mouse CD45 antibodies (Figure 1C,E). Although there was recipient-to-recipient variability, the frequency of human $CD33^+$ myeloid cells within the total human $CD45^+$ population was significantly higher in the hSCF Tg NSG recipient BM than in the non-Tg NSG recipient BM and constituted the majority of human hematopoietic cells (hSCF Tg: 49.7% ± 4.0%; n = 21 and non-Tg NSG controls: 26.2% ± 2.9%; n = 13; $P = .0002$ by 2-tailed t test). In contrast, in non-Tg NSG recipients, the majority of human hematopoietic cells in the BM were B cells (53.3% ± 4.5%; n = 13), consistent with previous reports.[5,9,20] These findings demonstrate that the expression of membrane-bound hSCF in BM microenvironment results in significantly more efficient engraftment of human HSCs as well as enhanced development of human $CD33^+$ myeloid cells from the engrafted human HSCs.

Human myeloid lineage development in hSCF Tg NSG recipients

Next, we examined the development of human myeloid subsets in the human membrane-bound SCF-expressing BM microenvironment. Flow cytometric scatter plots demonstrate the development of the SSC high granulocyte fraction in hSCF Tg NSG recipients, which correlate with $CD33^+HLA\text{-}DR^-$ cells (Figure 2A-B). To quantify the frequencies of different myeloid subsets in these recipients, we first identified $CD33^+c\text{-}Kit^+CD203c^+$ mature human mast cells among human $CD45^+$ cells. Next, we identified $CD33^+HLA\text{-}DR^-$ human granulocyte lineage cells and human $CD33^+HLA\text{-}DR^+$ antigen-presenting cells (APCs) among human $CD45^+$ cells excluding mature mast cells (Figure 2C).

In the hSCF Tg NSG recipient BM, there were increased percentages of $CD33^+HLA\text{-}DR^-$ granulocytes and decreased percentages of $CD33^+HLA\text{-}DR^+$ APCs compared with non-Tg NSG controls (hSCF Tg: 46.7% ± 5.9% and 38.3% ± 4.0%, respectively; n = 20 and non-Tg NSG controls: 25.8% ± 5.0% and 65.5% ± 4.1%, respectively; n = 12; $P = .0204$ and $P = .0001$ by 2-tailed t test, respectively; Figure 2D). In the BM of 11 of 20 hSCF Tg NSG recipients examined, $c\text{-}Kit^-CD203c^-HLA\text{-}DR^-$ SSC^{high} granulocytes accounted for the highest frequency of total human myeloid cells (Figure 2D; Table 1). To examine the morphologic features of the human granulocytes developing in the hSCF Tg recipients, we carried out May-Grünwald-Giemsa (MGG) staining using cytospin specimens of FACS-purified $CD33^+c\text{-}$

$Kit^-CD203c^-HLA\text{-}DR^-$ cells from BM of hSCF Tg and non-Tg NSG recipients. In 9 of 13 hSCF Tg recipient BM cells examined, the majority of myeloid cells showed the morphology of immature granulocytes with large nuclear-to-cytoplasmic ratio and nuclei with few lobulations, largely consisting of myelocytes and metamyelocytes (S4-1 and S12-2 shown as representative in Figure 2E). In 4 of 13 hSCF Tg recipients examined and in 4 of 5 non-Tg NSG recipients, mature segmented neutrophils were present in the sorted $CD33^+c\text{-}Kit^-CD203c^-HLA\text{-}DR^-$ granulocyte population (N12-1 and S2-1 shown as representative in Figure 2E). These findings indicate that both by quantitative and morphologic examinations, human granulocytic cells with various degrees of maturity predominate among the $CD33^+$ myeloid cells developing within the hSCF Tg NSG recipients. To examine the myeloid differentiation capacity of hematopoietic stem and progenitor populations in a functional manner, we performed a colony-forming cell assay using $CD34^+CD38^-$ and $CD34^+CD38^+$ cells derived from BM of hSCF Tg NSG recipients and non-Tg NSG recipients. In both cell populations, myeloid and erythroid colony formation were similar between hSCF Tg NSG and non-Tg NSG recipient BM (supplemental Figure 3).

We then analyzed global transcriptional profiles of $CD33^+HLA\text{-}DR^-c\text{-}Kit^-CD203c^-$ granulocytes from hSCF Tg NSG recipient BM (n = 4), non-Tg NSG recipient BM (n = 3), and primary human BM (n = 2). Additional control samples included BM monocytes from hSCF Tg recipients (n = 3), non-Tg NSG recipient BM monocytes (n = 3), and primary human BM monocytes (n = 2). Unsupervised clustering demonstrated a clear segregation of transcriptional profiles between granulocytes and monocytes regardless of the source. This suggests that human granulocytes and monocytes in humanized mouse undergo a distinct differentiation process similar to their counterparts in human BM (Figure 2F). We next examined whether there were any differences in gene expression within 3 distinct granulocyte sources (hSCF Tg recipient BM, non-Tg NSG recipient BM, and primary human BM neutrophils; Figure 2G). As seen in the heatmap representation, we found clusters of genes differentially transcribed in the distinct sources of granulocytes (Figure 2G). Multiple genes associated with transcriptional regulation were included in the genes upregulated in human immature granulocytes derived from the BM of hSCF Tg NSG mice, suggesting that these cells are more actively cycling and proliferating compared with mature granulocytes from the BM of hSCF Tg NSG and non-Tg NSG mice and primary human BM neutrophils (Figure 2G; supplemental Tables 1 and 2).

Development of human mast cells in hSCF Tg NSG recipients

We next investigated the development of human mast cells in the membrane-bound hSCF-expressing NSG mice. Overall, the frequencies of $cKit^+CD203c^+$ cells within total BM $CD33^+$ myeloid cells were similar between hSCF Tg NSG and non-Tg NSG recipients when excluding 2 non-Tg NSG recipients observed for more than 8 months ($P = .1439$ by 2-tailed t test; Figure 2D; Table 1). In 7 of 20 hSCF Tg NSG recipients, compared with one of 10 non-Tg NSG recipients, the frequency of $cKit^+CD203c^+$ cells in BM $CD33^+$ cells was greater than 15% (Figure 2D; Table 1). When these $cKit^+CD203c^+$ cells were FACS-purified and examined by MGG staining, their morphology was consistent with mast cells with various degrees of cytoplasmic granulation (Figure 3A-B). Histologic examination of H&E-stained bone sections showed increased cellularity in hSCF Tg NSG recipients compared with non-Tg NSG recipients (Figure 3C). We then performed IHC staining for mast cell tryptase to identify human mast cells in the BM. Consistent with the quantitative analysis by flow cytometry, $tryptase^+$ cells were abundantly observed in the hSCF Tg NSG recipients compared with non-Tg NSG recipients (Figure 3C). This does not reflect an increase in mouse mast cells because nearly all nucleated hematopoietic cells in the hSCF Tg NSG recipients are of human origin (Figure 1D). The same sections were further subjected to the immunofluorescence staining followed by confocal imaging demonstrating that these are mast cells and not $CD14^+$ monocytes (supplemental Figure 4).

Mast cell progenitors and mature mast cells reside in high frequencies in the spleen of normal immunocompetent mice.[21] We next examined the spleen of human HSC-engrafted hSCF Tg NSG recipients. Human $CD33^{high}c\text{-}Kit^+CD203c^+$ mast cells accounted for the highest frequency among total $hCD45^+hCD33^+$ myeloid cells in the spleen of both hSCF Tg NSG and non-Tg NSG HSC-engrafted recipients (Figure 4A-B). However, the frequencies of human mast cells in the myeloid cell population were significantly higher in hSCF Tg NSG recipients than in non-Tg NSG controls (hSCF Tg: 77.4% ± 4.5%; n = 20 and non-Tg NSG controls: 62.5% ± 3.9%; n = 12; $P = .0304$ by 2-tailed t test; Figure 4B). These human cells with surface expression phenotype of mast cells also showed morphologic features of mature mast cells (Figure 4C). Mast cell tryptase IHC staining confirmed the presence of human mast cells within the recipient spleen (Figure 4D). These findings indicate that the expression of membrane-bound human SCF in the recipient mouse microenvironment enhances development of human mast cells from transplanted human HSCs within hematopoietic organs, such as the BM and spleen, consistent with the activation of c-Kit signaling.

Next, we investigated whether the transgenic expression of hSCF results in the efficient development of mucosal tissue-type human mast cells in respiratory and gastrointestinal mucosal layers, as well as in hematopoietic organs. For this purpose, we performed IHC staining of human tryptase-expressing mast cells in the lung, stomach, small intestine, and large intestine in hSCF Tg NSG and non-Tg NSG recipients. In the hSCF Tg NSG recipient lungs, human tryptase-positive mast cells were identified within cellular infiltrates (supplemental Figure 5). In tissue sections from the stomach, small intestine, and large intestine, human tryptase-positive mast cells were present in both hSCF Tg NSG and non-Tg NSG recipients (Figure 5A-B). The mast cell $tryptase^+$ cells in gastrointestinal tissues of hSCF Tg mice were further examined by immunofluorescence microscopy using anti–human CD45 and anti–human-c-Kit antibodies. We found the presence of $hCD45^+c\text{-}Kit^+$ cells in the gastric tissues of the hSCF Tg recipients consistent with IHC staining for mast cell tryptase (Figure 5C). Because gastric tissue is one of the major sites of mast cell populations in humans and mice, we quantified human mast cells in the gastric tissue of hSCF Tg and non-Tg NSG recipients transplanted with human HSCs. IHC staining for human mast cell tryptase followed by quantification of $tryptase^+$ cells demonstrated the presence of human mast cells in gastric tissues of hSCF Tg NSG recipients (7.01% ± 0.63%, 3 sites per recipient analyzed in 3 mice) compared with non-Tg NSG recipients (2.53% ± 0.53%, 3 sites per recipient analyzed in 3 mice: $P < .0001$ by 2-tailed t test; Figure 5D). Collectively, transgenic expression of human membrane-bound SCF influences human myeloid development and mast cell development in hematopoietic organs and mucosal tissues along with the achievement of high chimerism of human hematopoietic cells in hematopoietic organs.

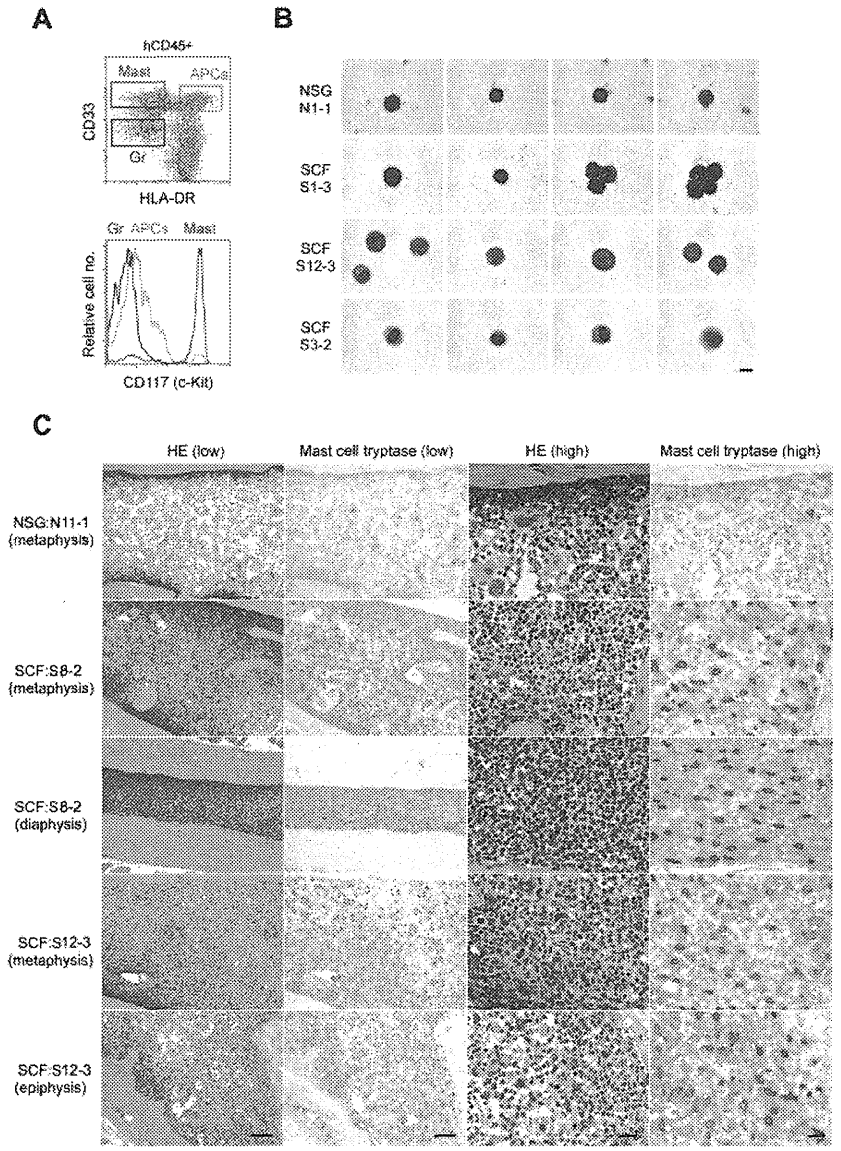

Figure 3. Human mast cell development in hSCF Tg NSG recipient BM. (A) Representative flow cytometric scatter plot and histogram demonstrating the identification of human $CD45^+CD33^+CD117^+$ mast cells. (B) FACS-sorted $hCD45^+CD33^+CD117^+CD203c^+$ human mast cells from a representative non-Tg NSG recipient BM (N1-1, 0.9% human mast cells within $hCD45^+CD33^+$ population) and hSCF Tg NSG recipient BM (S1-3, 14.6%; S12-3, 8.8%; and S3-2, 7.3% human mast cells within the $hCD45^+CD33^+$ population) were examined by MGG staining (N1-1, killed at 21 weeks; S1-3, killed at 21 weeks; S12-3, killed at 13 weeks; and S3-2, killed at 15 weeks). (C) H&E- and anti-mast cell tryptase antibody–stained bone sections demonstrate hypercellular BM with high frequency of $tryptase^+$ human mast cells in hSCF Tg NSG recipients. Non-Tg NSG recipient: N11-1, 70.7% $hCD45^+$. hSCF Tg NSG recipients: S8-2, 99.6%; and S12-3, 79.5% $hCD45^+$ (N11-1, killed at 20 weeks; S8-2, killed at 11 weeks; and S12-3, killed at 13 weeks).

Discussion

A supportive microenvironment is essential for hematopoietic and immune system homeostasis. Critical roles played by various niches in the maintenance of cell cycle quiescence and self-renewal capacity of HSCs have been demonstrated, and the thymic microenvironment is critical for T-cell education.[22,23] However, despite significant progress over the last decade, the stromal microenvironment within the humanized mouse is predominately of mouse origin. Although several key molecules, such as SDF1, are cross-reactive between human and mouse, a humanized microenvironment is required both to further improve human hematopoietic development in the recipients and to investigate in vivo the interactions between hematopoietic cells and their microenvironment.

In the present study, we humanized membrane-bound stem cell factor [SCF = KIT ligand (KL)] using the construct and mouse strain created by Majumdar et al.[13] Toksoz et al reported that human membrane-bound SCF expressed by mouse stromal cells efficiently supports long-term human hematopoiesis in vitro.[24] The importance of SCF interaction with $cKit^+$ HSCs and mast cell progenitors in murine hematopoiesis is highlighted by the hematopoietic abnormalities in mice with *Kitl* and *Kit* mutations.[25-27] In human hematopoiesis, SCF-cKit signaling is critical for the maintenance of stem and progenitor cell activities.[28] Human SCF/KL has been shown to drive cell-cycle entry by primitive hematopoietic cells in vitro.[29] Both long-term colony-initiation and colony-forming capacities are expanded ex vivo by cytokine supplementation that includes SCF/KL.[30-32] Therefore, to elucidate the role of membrane-bound human SCF in differentiation, proliferation, and maturation of human hematopoiesis in vivo, we created a novel NSG mouse strain that can support the engraftment of human HSCs and express hSCF in microenvironment. In hSCF Tg NSG recipients transplanted with human HSCs, the engraftment levels of human $CD45^+$ cells were significantly higher compared with non-Tg NSG controls. Majumdar et al reported that human SCF binds mouse c-Kit receptor but that the binding affinity is

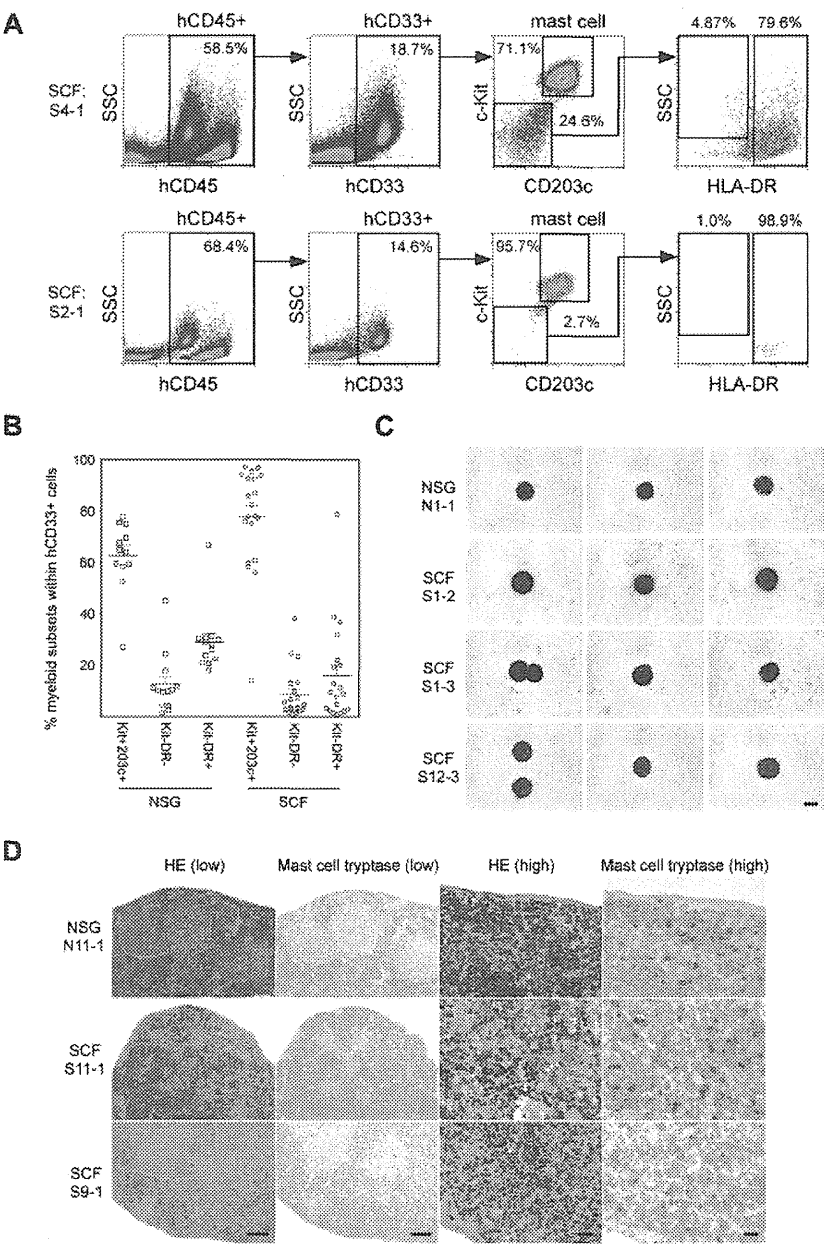

Figure 4. Human mast cell development in hSCF Tg NSG recipient spleen. (A) Human mast cell development is enhanced in hSCF Tg NSG recipient spleens (S4-1, killed at 13 weeks; and S2-1, killed at 16 weeks). (B) Frequencies of human c-Kit$^+$CD203c$^+$ mast cells, CD33$^+$HLA-DR$^-$ granulocyte population, and CD33$^+$HLA-DR$^+$ APCs within total hCD45$^+$hCD33$^+$ myeloid cells in the spleens of hSCF Tg and non-Tg NSG recipients. Human mast cell development in the spleen was significantly greater in the hSCF Tg NSG recipients (hSCF Tg: n = 20, non-Tg NSG: n = 12, $P = .0304$). (C) FACS-sorted hCD45$^+$CD33$^+$CD117$^+$CD203c$^+$ human mast cells from a representative non-Tg NSG recipient spleen (N1-1, 59.3% human mast cells within hCD45$^+$CD33$^+$ population) and hSCF Tg NSG recipient spleen (S1-2, 85.7%; S1-3, 77.7%; and S12-3, 56.1% human mast cells within hCD45$^+$CD33$^+$ population) were examined by MGG staining (N1-1, killed at 21 weeks; S1-2, killed at 20 weeks; S1-3, killed at 21 weeks; and S12-3, killed at 13 weeks). (D) H&E- and anti–mast cell tryptase antibody–stained spleen sections demonstrating the presence of human mast cells in non-Tg NSG recipients and hSCF Tg NSG recipients (non-Tg NSG recipient: N11-1, 94.0% hCD45$^+$; hSCF Tg NSG recipients: S11-1, 95.3%; and S9-1, 97.0% hCD45$^+$; N11-1, killed at 20 weeks; S11-1, killed at 10 weeks; and S9-1, killed at 16 weeks).

weaker compared with the binding affinity of human SCF to human c-Kit.[13] Therefore, the significant improvement of human hematopoietic chimerism could be attributed to preferential binding of human SCF to human HSCs instead of murine c-Kit$^+$ HSCs resulting in accelerated signaling through c-Kit in human HSCs and by impaired or attenuated support of mouse HSCs.[1,33,34] Presumably because of the competition between human and mouse hematopoietic stem or myeloid/erythroid progenitor cells, we observed diminished mouse erythrocyte hemoglobin concentration with normal range of mean corpuscular volume, mean corpuscular hemoglobin, and mean corpuscular hemoglobin concentration in all the 21 hSCF Tg NSG recipients but not in any of the non-Tg NSG recipients or nontransplanted hSCF Tg NSG adults. In addition to the greatly increased levels of human hematopoietic repopulation, we identified significant differences in human hematopoietic differentiation in hSCF Tg NSG recipients compared with non-Tg NSG recipients. Namely, there were substantially increased levels of human myeloid differentiation from HSCs in the hSCF Tg NSG mice, whereas human B cells accounted for the greatest population in the BM of non-Tg NSG mice. Because normal human BM contains myeloid cells at a relatively high frequency (36.2%-62.2%),[35] human SCF may be important in recapitulating human BM myelopoiesis in immunodeficient mice. In addition, membrane-bound human SCF may exert distinct effects on human myeloid development in the BM and in the spleen. In the BM of hSCF Tg recipients, the majority of human myeloid cells were c-Kit$^-$CD203c$^-$HLA-DR$^-$ granulocytes. Among these granulocytes, myeloid cells at various levels of maturity were identified, with myelocytes and metamyelocytes predominating in the majority of hSCF Tg NSG recipients. Because immature cells were more prominent in hSCF Tg NSG recipients compared with non-Tg NSG recipients, we performed microarray analysis to

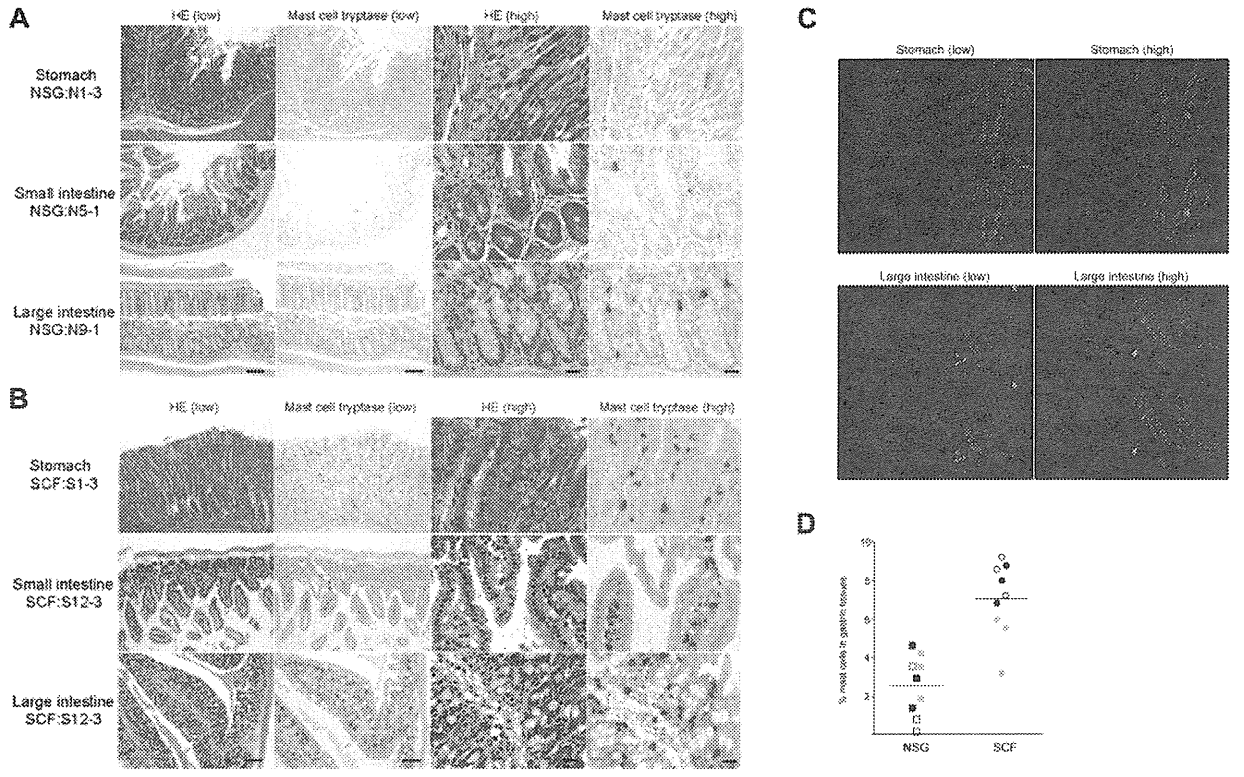

Figure 5. Human mast cell development in hSCF Tg NSG recipient stomach, small intestine, and large intestine. H&E- and anti–mast cell tryptase antibody–stained sections of (A) non-Tg NSG recipient stomach (NSG control, N1-3), small intestine (N5-1), and large intestine (N9-1) and (B) hSCF Tg NSG recipient stomach (S1-3), small intestine (S12-3), and large intestine (S12-3) demonstrating the presence of human mast cells (N1-3, killed at 24 weeks; N5-1, killed at 35 weeks; N9-1, killed at 20 weeks; S1-3, killed at 21 weeks; and S12-3, killed at 13 weeks). (C) Confocal immunofluorescence images of hSCF Tg stomach (S1-9) demonstrate human CD45$^+$ (green) and human CD117$^+$ (red) mast cells. (D) Frequencies of tryptase$^+$ cells were quantified by sampling 3 areas each from hSCF Tg (n = 3) and non-Tg (n = 3) NSG recipients: hSCF Tg NSG recipients, 7.0% ± 0.6%; and non-Tg NSG recipients, 2.5% ± 0.5% ($P < .0001$ by 2-tailed t test).

identify transcriptional signature specific to the immature human granulocytes that developed in the hSCF Tg NSG mice. Approximately 300 genes were differentially transcribed in the immature granulocytes in hSCF Tg NSG recipients compared with the mature granulocytes in non-Tg NSG recipients. Some of the up-regulated genes were associated with cell cycle or metabolism.

In several hSCF Tg NSG recipients, human mast cells composed the greatest subfraction among engrafted human myeloid cells. In the spleens of hSCF Tg NSG-engrafted mice, human mast cells were present at the highest frequency among the myeloid lineage developed in the recipients. MGG staining revealed both mature and immature mast cells in hSCF Tg NSG recipient BM. Human mast cells were identified not only in hematopoietic organs but also in lung, gastric tissue, and intestinal tissues of hSCF Tg NSG recipients. Aberrant expression of CD30 and CD25 on mast cells is associated with systemic mastocytosis and other mast cell disorders.[36,37] We did not find significantly up-regulated expression of these antigens in the mast cells derived from BM or spleen of hSCF Tg NSG recipients.

To date, several mouse strains have been developed for supporting normal and malignant human hematopoietic cell engraftment and normal myeloid cell differentiation using *Il2rg*^{null} immune-compromised mice (supplemental Table 3).[5,6,8,9,20,38-41] Among these, human thrombopoietin knock-in *Rag2*^{null} *Il2rg*^{null} mice were reported to support both human hematopoietic engraftment and myeloid differentiation in the BM. Both SCF and thrombopoietin exhibit species specificity between humans and mouse in supporting HSCs and myeloid cells in both species. These approaches focusing on the 2 distinct molecules based on the 2 immune-compromised mouse backgrounds will allow us to investigate human hematopoiesis and immunity from stem cells to myeloid progenitors to mature myeloid effecter cells in vivo. Altogether, the newly created hSCF Tg NSG mouse model engrafted with purified human HSCs will facilitate the in vivo understanding of human hematopoietic hierarchy and mast cell biology.

Acknowledgments

The authors thank David Williams for providing C3H/HeJ mice carrying the human SCF transgene and Dr Kodo and his staff at the Tokyo Cord Blood Bank for their generous assistance in processing and providing cord blood samples.

This work was supported by the National Institutes of Health (research grants HL077642, CA34196, AI46629, UO1 AI073871, DK089572), the University of Massachusetts Center for AIDS Research (P30 AI042845), the Juvenile Diabetes Foundation, International, the Helmsley Foundation, USAMRIID (L.D.S.), Project for Developing Innovation Systems, Program for Fostering Regional Innovation (O.O.), Takeda Science Foundation and Ministry of Education, Culture, Sports, Science and Technology, Japan (F.I.), and the Japan Society for the Promotion of Science through the Funding Program for Next Generation World-Leading Researchers (NEXT Program), initiated by the Council for Science and Technology Policy.

The contents of this publication are solely the responsibility of the authors and do not necessarily represent the official views of the National Institutes of Health.

Authorship

Contribution: S. Takagi, S. Tanaka, T.H., and S.M. performed the experiments; A.H., T.W., and O.O. performed and analyzed the microarray experiments; J.K., H. Kiyono, H. Koseki, O.O., T.S., and S. Taniguchi participated in discussions on research planning and analysis of results; and S. Takagi, Y.S., L.D.S., and F.I. designed the research and wrote the paper.

Conflict-of-interest disclosure: The authors declare no competing financial interests.

Correspondence: Fumihiko Ishikawa, Research Unit for Human Disease Models, RIKEN Research Center for Allergy and Immunology, 1-7-22 Suehiro-cho Tsurumi-ku, Yokohama, Kanagawa, Japan 230-0045; e-mail: f_ishika@rcai.riken.jp.

References

1. Manz MG. Human-hemato-lymphoid-system mice: opportunities and challenges. *Immunity.* 2007;26(5):537-541.
2. Shultz LD, Ishikawa F, Greiner DL. Humanized mice in translational biomedical research. *Nat Rev Immunol.* 2007;7(2):118-130.
3. McCune JM, Namikawa R, Kaneshima H, Shultz LD, Lieberman M, Weissman IL. The SCID-hu mouse: murine model for the analysis of human hematolymphoid differentiation and function. *Science.* 1988;241(4873):1632-1639.
4. Mosier DE, Gulizia RJ, Baird SM, Wilson DB. Transfer of a functional human immune system to mice with severe combined immunodeficiency. *Nature.* 1988;335(6187):256-259.
5. Ishikawa F, Yasukawa M, Lyons B, et al. Development of functional human blood and immune systems in NOD/SCID/IL2 receptor gamma chain(null) mice. *Blood.* 2005;106(5):1565-1573.
6. Ito M, Hiramatsu H, Kobayashi K, et al. NOD/SCID/gamma(c)(null) mouse: an excellent recipient mouse model for engraftment of human cells. *Blood.* 2002;100(9):3175-3182.
7. Shultz LD, Banuelos S, Lyons B, et al. NOD/LtSz-Rag1nullPfpnull mice: a new model system with increased levels of human peripheral leukocyte and hematopoietic stem-cell engraftment. *Transplantation.* 2003;76(7):1036-1042.
8. Shultz LD, Lyons BL, Burzenski LM, et al. Human lymphoid and myeloid cell development in NOD/LtSz-scid IL2R gamma null mice engrafted with mobilized human hemopoietic stem cells. *J Immunol.* 2005;174(10):6477-6489.
9. Traggiai E, Chicha L, Mazzucchelli L, et al. Development of a human adaptive immune system in cord blood cell-transplanted mice. *Science.* 2004; 304(5667):104-107.
10. Strowig T, Gurer C, Ploss A, et al. Priming of protective T cell responses against virus-induced tumors in mice with human immune system components. *J Exp Med.* 2009;206(6):1423-1434.
11. Jaiswal S, Pearson T, Friberg H, et al. Dengue virus infection and virus-specific HLA-A2 restricted immune responses in humanized NOD-scid IL2rgammanull mice. *PLoS One.* 2009;4(10): e7251.
12. Shultz LD, Saito Y, Najima Y, et al. Generation of functional human T-cell subsets with HLA-restricted immune responses in HLA class I expressing NOD/SCID/IL2r gamma(null) humanized mice. *Proc Natl Acad Sci U S A.* 2010; 107(29):13022-13027.
13. Majumdar MK, Everett ET, Xiao X, et al. Xenogeneic expression of human stem cell factor in transgenic mice mimics codominant c-kit mutations. *Blood.* 1996;87(8):3203-3211.
14. Hong F, Breitling R, McEntee CW, et al. RankProd: a bioconductor package for detecting differentially expressed genes in meta-analysis. *Bioinformatics.* 2006;22(22):2825-2827.
15. Draghici S, Khatri P, Martins RP, et al. Global functional profiling of gene expression. *Genomics.* 2003;81(2):98-104.
16. Benjamini Y, Hochberg Y, et al. Controlling the false discovery rate: a practical and powerful approach to multiple testing. *J R Stat Soc B Met.* 1995;57(1):289-300.
17. Kawashima I, Zanjani ED, Almaida-Porada G, Flake AW, Zeng H, Ogawa M. CD34+ human marrow cells that express low levels of Kit protein are enriched for long-term marrow-engrafting cells. *Blood.* 1996;87(10):4136-4142.
18. Sakabe H, Kimura T, Zeng Z, et al. Haematopoietic action of flt3 ligand on cord blood-derived CD34-positive cells expressing different levels of flt3 or c-kit tyrosine kinase receptor: comparison with stem cell factor. *Eur J Haematol.* 1998;60(5): 297-306.
19. Yoshikubo T, Inoue T, Noguchi M, Okabe H. Differentiation and maintenance of mast cells from CD34+ human cord blood cells. *Exp Hematol.* 2006;34(3):320-329.
20. Hiramatsu H, Nishikomori R, Heike T, et al. Complete reconstitution of human lymphocytes from cord blood CD34+ cells using the NOD/SCID/gammacnull mice model. *Blood.* 2003;102(3): 873-880.
21. Arinobu Y, Iwasaki H, Gurish MF, et al. Developmental checkpoints of the basophil/mast cell lineages in adult murine hematopoiesis. *Proc Natl Acad Sci U S A.* 2005;102(50):18105-18110.
22. Kiel MJ, Morrison SJ. Uncertainty in the niches that maintain haematopoietic stem cells. *Nat Rev Immunol.* 2008;8(4):290-301.
23. Jenkinson EJ, Jenkinson WE, Rossi SW, Anderson G. The thymus and T-cell commitment: the right niche for Notch? *Nat Rev Immunol.* 2006;6(7):551-555.
24. Toksoz D, Zsebo KM, Smith KA, et al. Support of human hematopoiesis in long-term bone marrow cultures by murine stromal cells selectively expressing the membrane-bound and secreted forms of the human homolog of the steel gene product, stem cell factor. *Proc Natl Acad Sci U S A.* 1992;89(16):7350-7354.
25. Besmer P, Manova K, Duttlinger R, et al. The kit-ligand (steel factor) and its receptor c-kit/W: pleiotropic roles in gametogenesis and melanogenesis. *Dev Suppl.* 1993;125-137.
26. Geissler EN, McFarland EC, Russell ES. Analysis of pleiotropism at the dominant white-spotting (W) locus of the house mouse: a description of ten new W alleles. *Genetics.* 1981;97(2):337-361.
27. Russell ES. Hereditary anemias of the mouse: a review for geneticists. *Adv Genet.* 1979;20:357-459.
28. Broudy VC. Stem cell factor and hematopoiesis. *Blood.* 1997;90(4):1345-1364.
29. Leary AG, Zeng HQ, Clark SC, Ogawa M. Growth factor requirements for survival in G0 and entry into the cell cycle of primitive human hemopoietic progenitors. *Proc Natl Acad Sci U S A.* 1992; 89(9):4013-4017.
30. Bernstein ID, Andrews RG, Zsebo KM. Recombinant human stem cell factor enhances the formation of colonies by CD34+ and CD34+lin− cells, and the generation of colony-forming cell progeny from CD34+lin− cells cultured with interleukin-3, granulocyte colony-stimulating factor, or granulocyte-macrophage colony-stimulating factor. *Blood.* 1991;77(11):2316-2321.
31. Haylock DN, To LB, Dowse TL, Juttner CA, Simmons PJ. Ex vivo expansion and maturation of peripheral blood CD34+ cells into the myeloid lineage. *Blood.* 1992;80(6):1405-1412.
32. Petzer AL, Hogge DE, Landsdorp PM, Reid DS, Eaves CJ. Self-renewal of primitive human hematopoietic cells (long-term-culture-initiating cells) in vitro and their expansion in defined medium. *Proc Natl Acad Sci U S A.* 1996;93(4):1470-1474.
33. Lev S, Yarden Y, Givol D. Dimerization and activation of the kit receptor by monovalent and bivalent binding of the stem cell factor. *J Biol Chem.* 1992;267(22):15970-15977.
34. Martin FH, Suggs SV, Langley KE, et al. Primary structure and functional expression of rat and human stem cell factor DNAs. *Cell.* 1990;63(1):203-211.
35. Terstappen LW, Safford M, Loken MR. Flow cytometric analysis of human bone marrow: III. Neutrophil maturation. *Leukemia.* 1990;4(9):657-663.
36. Pardanani A. Systemic mastocytosis in adults: 2011 update on diagnosis, risk stratification, and management. *Am J Hematol.* 2011;86(4):362-371.
37. Sotlar K, Cerny-Reiterer S, Petat-Dutter K, et al. Aberrant expression of CD30 in neoplastic mast cells in high-grade mastocytosis. *Mod Pathol.* 2011;24(4):585-595.
38. Rongvaux A, Willinger T, Takizawa H, et al. Human thrombopoietin knockin mice efficiently support human hematopoiesis in vivo. *Proc Natl Acad Sci U S A.* 2011;108(6):2378-2383.
39. Pearson T, Shultz LD, Miller D, et al. Non-obese diabetic-recombination activating gene-1 (NOD-Rag1 null) interleukin (IL)-2 receptor common gamma chain (IL2r gamma null) null mice: a radioresistant model for human lymphohaematopoietic engraftment. *Clin Exp Immunol.* 2008;154(2): 270-284.
40. Brehm MA, Cuthbert A, Yang C, et al. Parameters for establishing humanized mouse models to study human immunity: analysis of human hematopoietic stem cell engraftment in three immunodeficient strains of mice bearing the IL2rgamma(null) mutation. *Clin Immunol.* 2010;135(1):84-98.
41. Strowig T, Rongvaux A, Rathinam C, et al. Transgenic expression of human signal regulatory protein alpha in Rag2−/−gammac−/− mice improves engraftment of human hematopoietic cells in humanized mice. *Proc Natl Acad Sci U S A.* 2011;108(32):13218-13223.

Transplant Infectious Disease, ISSN 1398-2273

Rapidly progressive fatal hemorrhagic pneumonia caused by *Stenotrophomonas maltophilia* in hematologic malignancy

H. Araoka, T. Fujii, K. Izutsu, M. Kimura, A. Nishida, K. Ishiwata, N. Nakano, M. Tsuji, H. Yamamoto, Y. Asano-Mori, N. Uchida, A. Wake, S. Taniguchi, A. Yoneyama. Rapidly progressive fatal hemorrhagic pneumonia caused by *Stenotrophomonas maltophilia* in hematologic malignancy. Transpl Infect Dis 2012: **14**: 355–363.

Abstract: *Background.* Pneumonia caused by *Stenotrophomonas maltophilia* is rare, but can be lethal in severely immunocompromised patients. However, its clinical course remains unclear.
Patients and methods. Patients with pneumonia caused by *S. maltophilia* in Toranomon Hospital (890 beds, Tokyo, Japan) were reviewed retrospectively between April 2006 and March 2010.
Results. During the study period, 10 cases of *S. maltophilia* pneumonia were identified. Seven patients had acute myeloid leukemia, 2 had myelodysplastic syndrome, and 1 had malignant lymphoma. All patients developed symptoms after allogeneic hematopoietic stem cell transplantation (HSCT). Five patients received first cord blood transplantation (CBT), 4 patients received second CBT, and 1 patient received first peripheral blood stem cell transplantation (PBSCT). The overall incidence of *S. maltophilia* pneumonia among 508 patients who received HSCT during the period was 2.0%. The incidence was 0% (0/95) in patients after bone marrow transplantation, 0.8% (1/133) after PBSCT, and 3.2% (9/279) after CBT. Pneumonia developed a median of 13.5 days (range, 6–40) after transplantation. At onset, the median white blood cell count was 10/μL (range, 10–1900), and the median neutrophil count was 0/μL (range, 0–1720). In all patients, *S. maltophilia* bacteremia developed with bloody sputum or hemoptysis. The 28-day mortality rate was 100%; the median survival after onset of pneumonia was 2 days (range, 1–10).
Conclusions. Hemorrhagic *S. maltophilia* pneumonia rapidly progresses and is fatal in patients with hematologic malignancy. Attention should be particularly paid to the neutropenic phase early after HSCT or prolonged neutropenia due to engraftment failure. A prompt trimethoprim-sulfamethoxazole-based multidrug combination regimen should be considered to rescue suspected cases of *S. maltophilia* pneumonia in these severely immunosuppressed patients.

H. Araoka[1], T. Fujii[2], K. Izutsu[3], M. Kimura[1], A. Nishida[3], K. Ishiwata[3], N. Nakano[3], M. Tsuji[3], H. Yamamoto[3], Y. Asano-Mori[3], N. Uchida[3], A. Wake[3], S. Taniguchi[3], A. Yoneyama[1]

[1]Department of Infectious Diseases, Toranomon Hospital, Tokyo, Japan, [2]Department of Pathology, Toranomon Hospital, Tokyo, Japan, [3]Department of Hematology, Toranomon Hospital, Tokyo, Japan

Key words: *Stenotrophomonas maltophilia*; pneumonia; incidence; neutropenia; hematologic malignancy; hematopoietic stem cell transplantation

Correspondence to:
Hideki Araoka, MD
Department of Infectious Diseases
Toranomon Hospital
2-2-2 Toranomon, Minato-ku, Tokyo 105-8470, Japan
Tel: +81-3-3588-1111
Fax: +81-3-3582-7068
E-mail: h-araoka@toranomon.gr.jp

Received 9 July 2011, revised 6 October 2011, accepted for publication 19 October 2011

DOI: 10.1111/j.1399-3062.2011.00710.x
Transpl Infect Dis 2012: **14**: 355–363

Stenotrophomonas maltophilia is a low-virulent non-fermenting gram-negative bacillus that can be isolated from diverse environments such as an aquatic environment and soil, and it rarely causes respiratory infections in the healthy population. When *S. maltophilia* is detected on culture of an airway sample, it usually represents colonization or a carrier state. However, it has recently been recognized as a

pathogen of hemorrhagic pneumonia in severely immunocompromised patients (1–5). Once respiratory infections caused by *S. maltophilia* develop, the prognosis is considered to be poor because of the severe immunodeficiency of these patients. However, the clinical features of *S. maltophilia* pneumonia have not been fully clarified, and only a few case series of *S. maltophilia* pneumonia have been published. In this study, we summarize the clinical features of 10 patients with a definitive diagnosis of *S. maltophilia* hemorrhagic pneumonia.

Patients and methods

Medical records of patients with pneumonia caused by *S. maltophilia* in Toranomon Hospital (890 beds, Tokyo, Japan) between April 2006 and March 2010 (4 years) were retrospectively reviewed. *S. maltophilia* pneumonia was defined when all of the following 4 criteria were met: 1) Clinical symptoms of cough, sputum production, and fever; 2) dominant thin gram-negative bacilli were detected on Gram staining of a lower respiratory airway sample obtained from sputum, tracheobronchial aspirate or bronchoscopy; 3) *S. maltophilia* was cultured from a lower respiratory airway sample; and 4) a new shadow appeared on chest x-ray. The onset of *S. maltophilia* pneumonia was defined when both the clinical symptoms and the new shadow on chest x-ray were demonstrated.

Vitek system (bioMérieux, Marcy l'Etiole, France), Vitek2 system (bioMérieux), and MicroScan WalkAway 96 SI (Siemens Healthcare, Deerfield, Illinois, USA) were used for bacterial identification and drug sensitivity tests.

Immunohistochemical study was performed using the MACH-2 multiplex staining system (Biocare Medical, Concord, California, USA) according to manufacturer's instructions. A rabbit polyclonal anti-*S. maltophilia* antibody (AB-T065; Advanced Targeting Systems, San Diego, California, USA) was used at a 1/50 dilution. Anti-cytokeratin CAM5.2 antibody (Becton Dickinson Biosciences, San Jose, California, USA) was used to highlight epithelial cells.

Results

All 10 patients were diagnosed as having *S. maltophilia* pneumonia. There was no apparent outbreak of *S. maltophilia* infection throughout the study period. The clinical characteristics of the 10 patients are shown in Tables 1 and 2.

There were 6 men and 4 women, with a median age of 58 years (range, 36–62). Underlying diseases were acute myeloid leukemia in 7 patients, myelodysplastic syndrome in 2 patients, and diffuse large B-cell lymphoma in 1 patient. All patients had already undergone allogeneic hematopoietic stem cell transplantation (HSCT). Five patients received first cord blood transplantation (CBT), 4 patients received second CBT, and 1 patient received first peripheral blood stem cell transplantation (PBSCT) (Table 1). All patients underwent transplantation in a non-remission state. During the study period, HSCT was performed in 508 patients (bone marrow transplantation [BMT]: 95, PBSCT: 133, CBT: 279, PBSCT + BMT: 1, and first HSCT: 366, second HSCT: 112, $\geq$ third HSCT: 30), and the overall incidence of *S. maltophilia* pneumonia was 2.0%. The incidence was 0% (0/95) in patients after BMT, 0.8% (1/133) after PBSCT, and 3.2% (9/279) with CBT. *S. maltophilia* pneumonia developed only in the HSCT setting, and no case of *S. maltophilia* pneumonia occurred among patients without hematologic disorders.

With respect to clinical characteristics that predisposed the patients to developing *S. maltophilia* pneumonia, they had been generally heavily pretreated before HSCT. Most patients had received >2 lines of chemotherapy before HSCT, and median length of hospital stay before HSCT was 123 days (range, 49–412). All patients had previously received broad-spectrum antimicrobial therapy including carbapenem and prophylactic fluoroquinolone in the 90 days before HSCT. Graft-versus-host disease (GVHD) prophylaxis consisted of tacrolimus and mycophenolate mofetil in 8 and tacrolimus alone in 2 patients. Corticosteroid had been used for GVHD or pre-engraftment immune reactions in 5 patients with a diagnosis of *S. maltophilia* pneumonia (Table 1). All patients had preparative regimen-related mucositis (grade $\geq$ 2 according to the National Cancer Institute Common Terminology Criteria for Adverse Events, version 4.0). Similarly, 9/10 patients had diarrhea (grade $\geq$ 1) due to preparative regimen and/or GVHD at the diagnosis of *S. maltophilia* pneumonia. However, no patients had apparent *Clostridium difficile*-associated disease.

The median onset of *S. maltophilia* pneumonia was 13.5 days (range, 6–40) after transplantation, and the median white blood cell and neutrophil counts at the time of onset were 10/μL (range, 10–1900) and 0/μL (range, 0–1720), respectively (Table 1). Pneumonia developed during broad-spectrum antibiotic treatment including fluoroquinolones in all patients. *S. maltophilia* was detected in airway samples before pneumonia onset in 3 patients (Patients 3, 4, and 10) (Table 1).

Clinical characteristics of the 10 patients with *Stenotrophomonas maltophilia* pneumonia (background)

Patient No.	Age (years)	Gender	Diagnosis	Transplantation	GVHD prophylaxis	Corticosteroid	White blood cell count (/μL)	Neutrophil count (/μL)	Time of onset after transplantation (days)	Pretreatment with antibiotics	Carrier state
1	45	M	AML	2nd CBT	TAC+MMF	No	20	0	11	MEPM, VCM	No
2	62	M	AML	CBT	TAC+MMF	No	10	0	6	PIPC/TAZ, CPFX, VCM	No
3	57	M	AML	Allo-PBSCT	TAC+MMF	No	1900	1720	27	CPFX	Yes
4	36	M	AML	2nd CBT	TAC+MMF	No	10	0	7	PAPM/BP, VCM	Yes
5	59	M	NHL	CBT	TAC	Methylprednisolone 125 mg	150		16	PIPC/TAZ, AZT, VCM	No
6	60	M	AML	CBT	TAC+MMF	Hydrocortisone 150 mg	10	0	7	PAPM/BP, VCM	No
7	56	F	AML	2nd CBT	TAC+MMF	Methylprednisolone 20 mg	10	0	34	CFPM, VCM	No
8	42	F	MDS	CBT	TAC+MMF	Methylprednisolone 40 mg	10	0	7	MEPM, VCM	No
9	59	F	AML	2nd CBT	TAC	Methylprednisolone 40 mg	310	78	25	MEPM, CPFX, AMK, VCM	No
10	62	F	MDS	CBT	TAC+MMF	No	10	0	40	PIPC/TAZ, GM, VCM	Yes

GVHD, graft-versus-host disease; M, male; F, female; AML, acute myeloid leukemia; NHL, non-Hodgkin lymphoma; MDS, myelodysplastic syndrome; CBT, cord blood transplantation; Allo-PBSCT, allogeneic peripheral blood stem cell transplantation; TAC, tacrolimus; MMF, mycophenolate mofetil; MEPM, meropenem; VCM, vancomycin; PIPC/TAZ, piperacillin/tazobactam; CPFX, ciprofloxacin; PAPM/BP, panipenem/betamipron; AZT, aztreonam; CFPM, cefepime; AMK, amikacin; GM, gentamicin.

Table 1

Clinical characteristics of the 10 patients with *Stenotrophomonas maltophilia* pneumonia (diagnosis and treatment)

					Treatment		
Patient No.	Blood culture	Mixed infection blood culture	Respiratory cultures except *S.maltophilia*	Time of death after onset (days)	TMP-SMX (Dose of TMP)	CCr (mL/min)	Fluoroquinolone
1	Positive	No	–	1	–	30	–
2	Positive	No	–	3	320 mg after HD	HD	Yes
3	Positive	No	*Enterococcus faecalis, Enterococcus faecium, Elizabethkingia meningoseptica*	10	400 mg after HD	HD	Yes
4	Positive	*Enterococcus* species	–	2	–	41	Yes
5	Positive	No	–	1	–	HD	–
6	Positive	*Enterococcus faecium*	–	2	320 mg/day	77	Yes
7	Positive	*Enterococcus faecium*	–	1	–	55	–
8	Positive	No	*Aspergillus* species	4	320 mg/day	40	Yes
9	Positive	No	*Enterococcus faecalis, Enterococcus faecium*	3	320 mg/day	16	Yes
10	Positive	*Citrobacter freundii*	–	1	720 mg/day	92	Yes

TMP-SMX, trimethoprim-sulfamethoxazole; HD, hemodialysis; CCr, creatinine clearance.

Table 2

Three patients (Patients 2, 3, and 5) received treatment with mechanical ventilation when pneumonia developed.

All patients had *S. maltophilia* bacteremia. Bacteria other than *S. maltophilia* were simultaneously detected on blood culture in 4 patients: Enterococci in 3 (*Enterococcus faecium*: 2, *Enterococcus* species: 1) and *Citrobacter freundii* in 1 (Table 2).

Bloody sputum or hemoptysis was noted in all patients. As shown in Figure 1A, red blood cells and many thin gram-negative bacilli were present in airway samples in all patients. Seven of 10 patients had pure *S. maltophilia* pneumonia, and only *S. maltophilia* was cultured from respiratory secretions. In the other 3 patients, other bacteria were cultured, but these bacteria were not observed on Gram stain finding, suggesting bacterial colonization in the airway. Also, these bacteria had low pathogenicity, except *Aspergillus* species (Patient 8) (Table 2). Two patients had fungal infection (*Candida glabrata*, *Aspergillus* species). No patients had apparent viral infection.

Chest computed tomography findings in Patient 6 are shown in Figure 2. Infiltrating shadows rapidly progressed within a very short period. Autopsy was performed in Patient 6. The lungs (weight 1110/1450 g) were voluminous with hemorrhage and edema. Microscopically, the lungs showed diffuse alveolar hemorrhage with the alveolar spaces filled with abundant extravasated blood and fibrinous exudate; the alveolar epithelial cells were widely disrupted and detached from the alveolar septa. There were some areas showing focal collapse due to fibrosis with hemosiderosis. Arterial and capillary vascular structures were retained, and no evidence of vasculitis or capillaritis was noted. The presence of *S. maltophilia* was clearly demonstrated on immunohistochemistry as shown in Figure 1B–F.

The mortality rate from *S. maltophilia* pneumonia was 100%. Although empiric or Gram staining-guided preemptive higher doses of trimethoprim-sulfamethoxazole (TMP-SMX) and fluoroquinolones with multiple broad-spectrum antibiotics were administered in 6 of the 10 patients, all of these patients died within a very

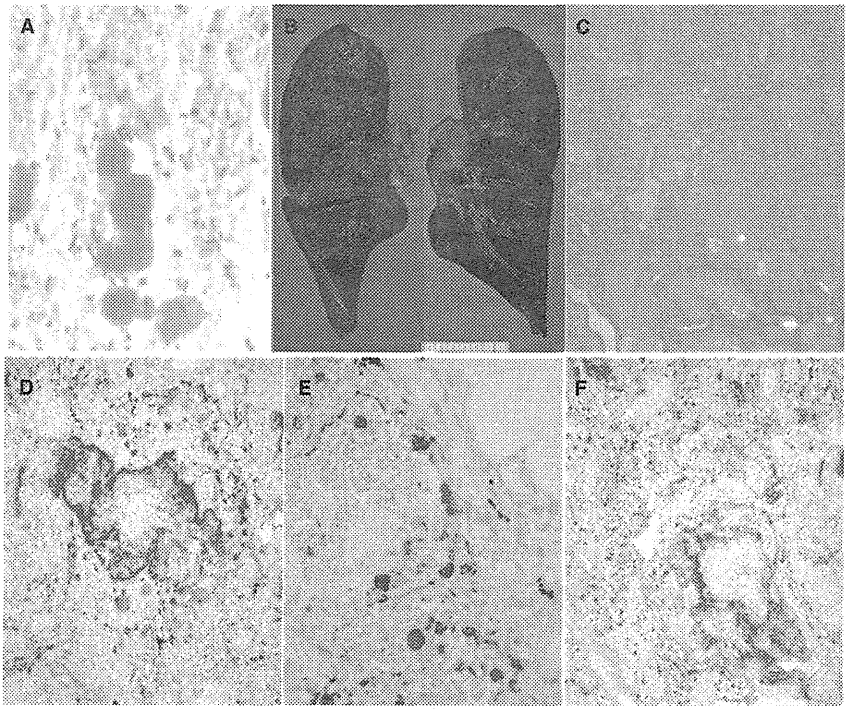

Fig. 1. *Stenotrophomonas maltophilia* pneumonia developed in a neutropenic state after cord blood transplantation. Bronchoalveolar lavage showed a red color, suggesting alveolar hemorrhage. Large amounts of red blood cells and thin gram-negative bacilli were found on Gram staining (A). Lungs obtained at autopsy demonstrated the presence of diffuse alveolar hemorrhage macroscopically (B) and histologically (C; hematoxylin-eosin, ×41) (Patient 6). Double immunohistochemical staining of the lung (D: ×83; E: ×165, F: ×41) showed the presence of *S. maltophilia* (red) located within/along the alveolar spaces filled with abundant extravasated blood/fibrinous exudate and widely disrupted alveolar epithelial cells (brown). In addition, the presence of macrophages phagocytizing *S. maltophilia* are noted.

Fig. 2. Patient 6 underwent cord blood transplantation for acute leukemia. Pneumonia developed when the neutrophil count was 0/μL on day 7 after transplantation. Compared with chest computed tomography on day 7 after transplantation (left), consolidation accompanied by an air bronchogram showed rapid expansion in the right lung field on the following day (day 8) (right).

short time after pneumonia onset (median: 2 days; range, 1–10) (Table 2). Regarding drug sensitivity, *S. maltophilia* was susceptible to TMP-SMX in all patients excluding Patient 6. The susceptibility rates to levofloxacin, minocycline, and ceftazidime were 70%, 100%, and 20%, respectively.

Discussion

Low-virulent multidrug-resistant *S. maltophilia* with low pathogenicity has been increasingly isolated with the development of immunosuppressive anti-cancer treatment including HSCT. Safdar and Rolston (6) reported that the ratio of gram-negative bacteria isolated from cancer patients was 2% in 1986, but accounted for 7% in 2002. However, it remains unclear whether the isolation frequency has steadily increased, because the isolation rate depends on local factors at each hospital (7). *S. maltophilia* has low virulence in healthy populations, but it is pathogenic in profoundly immunosuppressed patients. In general, *S. maltophilia* cultured from lower respiratory airway samples comprise mostly bacteria that have colonized the airway. When *S. maltophilia* is isolated from lower respiratory airway samples, it is difficult to differentiate infection from colonization. To diagnose *S. maltophilia* pneumonia, quantitative culture of bronchoalveolar lavage may be useful, but it has a limitation (8). To date, there has been limited literature describing the epidemiology of *S. maltophilia* pneumonia. A previous report showed that *S. maltophilia* accounted for 4.5% of hospital-acquired pneumonia cases and 6% of ventilator-associated pneumonia (9). Also, Jones (10) reported that *S. maltophilia* was isolated from 3.1% of patients hospitalized with pneumonia in the last 5 years of the SENTRY Antimicrobial Surveillance Program. However, the true incidence of *S. maltophilia* pneumonia could be much lower because that report included cases demonstrating colonization of *S. maltophilia* in the respiratory tract. We consider that Gram staining of lower respiratory airway samples is important. When dominant thin gram-negative bacilli are observed under a microscope and *S. maltophilia* is detected in culture, it is likely to be a true pathogen. We incorporated Gram stain findings into the diagnostic criteria of *S. maltophilia* pneumonia to exclude the cases of *S. maltophilia* colonization and improve the accuracy of diagnosis. However, it is possible that severe cases were selected, whereas mild to moderate cases that could be cured with antimicrobial therapy were excluded by these criteria.

This is the first report, to our knowledge, describing the incidence of *S. maltophilia* pneumonia in HSCT recipients. The majority of the patient population was CBT recipients, and the incidence of *S. maltophilia* pneumonia in CBT recipients tended to be higher compared with that in BMT and PBSCT recipients. The retrospective nature of this study is a limitation, as in other studies, and our study did not sufficiently exclude *S. maltophilia* cross-transmission. Thus, the true incidence of *S. maltophilia* pneumonia still remains unknown. However, no apparent outbreak occurred during the study period.

Regarding risk factors for *S. maltophilia* pneumonia, various studies mainly reported the following factors: 1) neutropenia; 2) hematologic malignancy, such as leukemia and malignant lymphoma; 3) patients treated with broad-spectrum antibiotics (carbapenems, broad-spectrum cephalosporins, and fluoroquinolones); 4) prolonged mechanical ventilation for 7 days or longer, or tracheotomy; and 5) anatomic abnormality in the trachea or lung, such as cystic fibrosis and chronic obstructive pulmonary disease (3, 6, 11).

Hemorrhagic pneumonia in patients with hematologic malignancy accompanied by neutropenia is a

characteristic pathological condition of *S. maltophilia* pneumonia, and it has been reported to cause alveolar hemorrhage and rapidly result in death (1–5). In our study, the disease developed with severe neutropenia in 9 of 10 patients, and occurred during the early phase after HSCT or prolonged neutropenia due to engraftment failure. Many of these patients had bloody sputum or hemoptysis. Clinicians should not overlook these clinical signs, although they may be lacking in the early stage of pneumonia, which should receive attention. In our series, 4 patients did not receive TMP-SMX-based multidrug combination treatment for *S. maltophilia,* because it was diagnosed after death. In these 4 patients, the median time of death after onset was only 1 day (range, 1–2). Reportedly, bacterial colonization is observed in the airway before the development of pneumonia in many cases, but in the presence of neutropenia, it may rapidly develop in the absence of confirming colonization. Indeed, colonization had been detected in only 3 of the 10 patients before the onset of *S. maltophilia* pneumonia.

Reportedly, images of *S. maltophilia* pneumonia did not show any characteristic feature compared with those of common bacterial pneumonia. It may show a uni- or bilateral pattern, but is rarely accompanied by pleural effusion (3, 11). Cavernous lesions are also rare. In patients with hematologic malignancy accompanied by neutropenia, particularly patients after HSCT, it may show rapid progression accompanied by hemorrhagic pneumonia. On imaging, early changes are minute in many cases, requiring careful observation. The detailed mechanism of alveolar hemorrhage has not been clarified, and further studies are necessary.

The mortality rate from *S. maltophilia* pneumonia is high, being reported to be 23–77% (12), and further increases in cases accompanied by *S. maltophilia* bacteremia (13). The blood culture positivity rate rises in the presence of neutropenia, and the mortality rate of such cases is very high. In severely immunocompromised patients who have profound neutropenia, mucositis, or presence of a catheter, multiple pathogens are often present, and the prognosis is poor (13). For such cases, blood culture to determine pathogens is very important. We also noted combined bacteremia in 4 of the 10 patients. It was reported that early catheter removal led to a better prognosis in the case of catheter-related *S. maltophilia* bacteremia (13).

In our study, the mortality rate of *S. maltophilia* pneumonia was higher than that in previous reports. This could have been due to the fact that 9 of the 10 patients received CBT and had prolonged severe neutropenia; furthermore, all 10 patients underwent transplantation in a non-remission state. It may be difficult to rescue patients when bacteria are shown in lower respiratory airway samples on Gram staining despite prompt treatment with TMP-SMX alone or TMP-SMX-based multidrug regimen, as observed in our cases. Patient 3, who received PBSCT and had a relatively shorter neutropenic period, had longer survival, indicating the essential role of neutrophils to manage *S. maltophilia* pneumonia. The prevention and early diagnosis of disease development need to be investigated.

S. maltophilia exhibits intrinsic resistance to a wide variety of antibiotics. It is resistant to most β-lactams including carbapenems by producing the L1- (class B metallo β-lactamase) and L2-type (class A) β-lactamases (14, 15); fluoroquinolones through a drug efflux pump, or reducing the outer membrane permeability to drugs (16, 17); and aminoglycosides by producing an aminoglycoside-modifying enzyme and through a drug efflux pump (6, 18–20). In previous reports, sensitivity to TMP-SMX and minocycline was high, but sensitivity to other drugs varied among reports (6). Treatment with TMP-SMX alone or TMP-SMX-based multidrug regimen (combination with ticarcillin clavulanate and/or fluoroquinolones) is considered the first choice (21–24). Treatment with TMP-SMX and fluoroquinolones is the only treatment option for *S. maltophilia* pneumonia in severely immunocompromised patients, as ticarcillin clavulanate has not been approved, and is not commercially available in Japan. However, treatment of *S. maltophilia* pneumonia without ticarcillin clavulanate would be disadvantageous because many patients at risk are likely to have fluoroquinolone prophylaxis, predisposing patients to fluoroquinolone-resistant *S. maltophilia* infection.

Regarding the dose of TMP-SMX, no clear data are available. As its action on *S. maltophilia* is considered bacteriostatic (25), higher dose may be recommended, as is the case for *Pneumocystis* pneumonia (15 mg/kg/day of trimethoprim) (26), but no prospective study data are available.

As most patients had not achieved neutrophil engraftment, none of them received prophylactic administration of TMP-SMX. A negative influence of TMP-SMX is a concern of clinicians engaged in HSCT because the prophylactic administration of TMP-SMX inhibits engraftment of hematopoietic stem cells. Prophylactic oral TMP-SMX administration between the transplantation day and neutrophil engraftment is not incorporated into common practice (27). It remains unclear whether TMP-SMX can prevent

S. maltophilia pneumonia and sepsis at the oral prophylactic dose for *Pneumocystis* pneumonia. Moreover, it remains unclear whether high-dose TMP-SMX negatively influences neutrophil engraftment when *S. maltophilia* pneumonia or sepsis develops before engraftment. However, a prompt TMP-SMX-based multidrug combination regimen should be considered to rescue suspected cases of *S. maltophilia* pneumonia in severely immunocompromised patients after HSCT. Further investigation is needed regarding the adequacy of the prophylactic administration of TMP-SMX before neutrophil engraftment after HSCT, particularly CBT, for which the incidence was the highest.

Conclusion

Hemorrhagic *S. maltophilia* pneumonia is rapidly progressive and associated with a high mortality rate in patients with hematologic malignancy. Attention should be particularly paid to the neutropenic phase early after HSCT or prolonged neutropenia due to engraftment failure. A prompt TMP-SMX-based multidrug combination regimen should be considered to rescue suspected cases of *S. maltophilia* pneumonia in these severely immunosuppressed patients. Considering the early mortality of our cohort, the prevention and early diagnosis of hemorrhagic *S. maltophilia* pneumonia will require further investigation.

Acknowledgements:

The authors thank data coordinators Kaori Kobayashi, Madoka Narita, Rumiko Tsuchihashi, and Naomi Yamada for their invaluable assistance. The authors also thank all physicians, nurses, pharmacists, and support personnel for their care of patients in this study.

Funding: This work was supported in part by a Research Grant from Okinaka Memorial Institute for Medical Research, Tokyo, Japan.

Disclosures: The authors have no conflict of interests to disclose.

References

1. Ortín X, Jaen-Martinez J, Rodríguez-Luaces M, Alvaro T, Font L. Fatal pulmonary hemorrhage in a patient with myelodysplastic syndrome and fulminant pneumonia caused by *Stenotrophomonas maltophilia*. Infection 2007; 35 (3): 201–202.
2. Pathmanathan A, Waterer GW. Significance of positive *Stenotrophomonas maltophilia* culture in acute respiratory tract infection. Eur Respir J 2005; 25 (5): 911–914.
3. Fujita J, Yamadori I, Xu G, et al. Clinical features of *Stenotrophomonas maltophilia* pneumonia in immunocompromised patients. Resp Med 1996; 90 (1): 35–38.
4. Elsner HA, Dührsen U, Hollwitz B, Kaulfers PM, Hossfeld DK. Fatal pulmonary hemorrhage in patients with acute leukemia and fulminant pneumonia caused by *Stenotrophomonas maltophilia*. Ann Hematol 1997; 74 (4): 155–161.
5. Takahashi N, Yoshioka T, Kameoka Y, et al. Fatal hemorrhagic pneumonia caused by *Stenotrophomanas maltophilia* in a patient with non-Hodgkin lymphoma. J Infect Chemother 2011; 17 (6): 858–862.
6. Safdar A, Rolston KV. *Stenotrophomonas maltophilia*: changing spectrum of a serious bacterial pathogen in patients with cancer. Clin Infect Dis 2007; 45 (12): 1602–1609.
7. Meyer E, Schwab F, Gastmeier P, Ruden H, Daschner FD. Is the prevalence of *Stenotrophomonas maltophilia* isolation and nosocomial infection increasing in intensive care units? Eur J Clin Microbiol Infect Dis 2006; 25 (11): 711–714.
8. Fujitani S, Yu VL. Quantitative cultures for diagnosing ventilator-associated pneumonia: a critique. Clin Infect Dis 2006; 43 (Suppl 2): S106–S113.
9. Weber DJ, Rutala WA, Sickbert-Bennett EE, Samsa GP, Brown V, Niederman MS. Microbiology of ventilator-associated pneumonia compared with that of hospital-acquired pneumonia. Infect Control Hosp Epidemiol 2007; 28 (7): 825–831.
10. Jones RN. Microbial etiologies of hospital-acquired bacterial pneumonia and ventilator-associated bacterial pneumonia. Clin Infect Dis 2010; 51 (Suppl 1): S81–S87.
11. Vartivarian SE, Anaissie EJ, Kiwan EN, Papadakis KA. The clinical spectrum of *Stenotrophomonas (Xanthomonas) maltophilia* respiratory infection. Sem Resp Crit Care Med 2000; 21 (4): 349–355.
12. Looney WJ, Narita M, Mühlemann K. *Stenotrophomonas maltophilia*: an emerging opportunist human pathogen. Lancet Infect Dis 2009; 9 (5): 312–323.
13. Araoka H, Baba M, Yoneyama A. Risk factors for mortality among patients with *Stenotrophomonas maltophilia* bacteremia in Tokyo, Japan, 1996–2009. Eur J Clin Microbiol Infect Dis 2010; 29 (5): 605–608.
14. Avison MB, Higgins CS, von Heldreich CJ, Bennett PM, Walsh TR. Plasmid location and molecular heterogeneity of the L1 and L2 beta-lactamase genes of *Stenotrophomonas maltophilia*. Antimicrob Agents Chemother 2001; 45 (2): 413–419.
15. Walsh TR, MacGowan AP, Bennett PM. Sequence analysis and enzyme kinetics of the L2 serine beta-lactamase from *Stenotrophomonas maltophilia*. Antimicrob Agents Chemother 1997; 41 (7): 1460–1464.
16. Alonso A, Martínez JL. Cloning and characterization of SmeDEF, a novel multidrug efflux pump from *Stenotrophomonas maltophilia*. Antimicrob Agents Chemother 2000; 44 (11): 3079–3086.
17. Ba BB, Feghali H, Arpin C, Saux MC, Quentin C. Activities of ciprofloxacin and moxifloxacin against *Stenotrophomonas maltophilia* and emergence of resistant mutants in an *in vitro* pharmacokinetic-pharmacodynamic model. Antimicrob Agents Chemother 2004; 48 (3): 946–953.
18. Okazaki A, Avison MB. Aph(3')-IIc, an aminoglycoside resistance determinant from *Stenotrophomonas maltophilia*. Antimicrob Agents Chemother 2007; 51 (1): 359–360.